C.P. No. 1283

C.P. No. 1283

PROCUREMENT EXECUTIVE, MINISTRY OF DEFENCE

AERONAUTICAL RESEARCH COUNCIL

CURRENT PAPERS

Results of a Series of Wind Tunnel Tests on the Victor B.Mk.2 Aircraft and a Comparison with Drag Estimates and Full Scale Flight Data

by

J. I. Simper,

Aircraft Research Association Ltd.,

with a Foreword by A. B. Haines

LONDON: HER MAJESTY'S STATIONERY OFFICE

1974

PRICE 85p NET

CP No.1283*
October, 1971

RESULTS OF A SERIES OF WIND TUNNEL TESTS ON THE VICTOR B.Mk.2 AIRCRAFT AND A COMPARISON WITH DRAG ESTIMATES AND FULL SCALE FLIGHT DATA

- by -
J. I. Simper,
Aircraft Research Association Ltd.

SUMMARY

Wind tunnel measurements of drag for a 1/25 scale model of the Victor B.Mk.2 have been compared with estimates and flight data.

At wind tunnel Reynolds numbers reasonable agreement is shown to exist between the estimated drag and an extrapolation to $M = 0$, $C_L = 0$ from the lowest test Mach number and moderate C_L, of the measured complete model drag.

At full scale Reynolds numbers the standard of agreement between the extrapolated wind tunnel and full scale flight drag data is shown to depend on whether the wind tunnel or flight derived η_{trim} values are used and the assumed drag of small excrescences not represented on the model. If certain assumptions are made then (1) at low and moderate C_L good agreement is shown to exist between the extrapolated wind tunnel and flight measured drags and (2) the wind tunnel tends to predict a later drag-rise than that measured in flight by $\Delta M = 0.015$ or less depending on the assumptions made.

Part of the analysis in this report was covered by Ministry of Technology Contract KC/49/25/CB5D.

---

*Replaces A.R.C.33 227

RESULTS OF A SERIES OF WIND TUNNEL TESTS ON THE VICTOR B.Mk.2 AIRCRAFT AND A COMPARISON WITH DRAG ESTIMATES AND FULL SCALE FLIGHT DATA

FOREWORD

by

A.B.Haines

Various factors limit the usefulness of this flight/tunnel drag comparison for the Victor B.Mk.2 but, as will be seen later, there are also factors of special value. The main limitations are,

(i) the flight data are not as extensive or as accurate as one would really like for a meticulous drag comparison exercise. The most reliable data are the 10 points which provide a Mach-number traverse at $C_L = 0.35$ and a C_L - traverse at $M = 0.819$ i.e. the specific data points plotted on figures 10(a,b). These were obtained by the quasi-level flight technique in which the aircraft is held as close to a given Mach number as possible having set the engine power for a given W/p or C_L and then measuring any resultant acceleration and/or climb from continuous recorder traces. It is considered that these 10 points should be accurate to within ± 0.0005 in C_D. Lower quality data from normal "engineering" tests in which the aircraft was flown at nominally steady conditions for sustained periods were used to define the shape of the lines in the carpet plot of C_D - M - C_L in figure 8. Admittedly, the quasi-level data were still the basis of the absolute values of C_D in figure 9 and hence of the C_D - M flight/tunnel comparisons for $C_L \neq 0.35$ in figure 11 but clearly, judgements on the flight/tunnel comparison should be based primarily on figure 10,

(ii) there is a significant difference between the elevator angles to trim as derived from the tunnel and flight tests. The considered judgement of those involved in the comparison was that the aeroelastic bending of the fuselage in flight had not been estimated correctly and that therefore, it was the flight values that were in error. However, this point was never proved conclusively and so, some uncertainty remains as to what is the true interpretation of the discrepancies. It is an important issue in the present context because the tunnel data show that if one chose to accept the flight rather than the tunnel elevator angles to trim, the Mach numbers for the rapid drag rise in the tunnel would be reduced by between 0.005 and 0.01,

In the light of (i, ii) and various other small points, the flight/tunnel drag comparison is inevitably less successful than other recent comparisons for the Trident[1] and BAC 1-11[2]. It is nevertheless being published on the grounds that

(a) it is the only one of the three comparisons where the flight data extends to a Mach number notably in excess of the value corresponding to the start of the steep drag-rise,

(b) even just to highlight the difficulties and problems involved in obtaining a reliable flight/tunnel comparison is in itself a useful task as a reminder of the care and effort that is needed if one is going to have any chance of drawing conclusions of general value,

(c) the main apparent conclusion from the comparison viz. that the Mach number for the steep drag-rise is higher in the model tests than in flight by about 0.01 at $C_L = 0.35$ and more than this at higher C_L, is an indication of the need to continue to try and obtain validated comparisons despite the difficulties. The conclusion for $C_L = 0.35$ is based on the quasi-level flight test data plotted in figure 10(b); no interpretation of the data within the accuracy stated under (i) above would produce agreement between flight and tunnel. On the other hand, the comparison is critically dependent on (ii); use of the elevator angles of trim from the tunnel tests would largely remove the discrepancy at $C_L = 0.35$. As noted in the last paragraph of the report on page 13, the results as presented suggest an adverse scale effect on the drag-divergence Mach number (M_D) but in view of the doubts, the precise magnitude and even the existence of this scale effect are uncertain. It is however fair to point out that a similar scale effect, again amounting to about 0.01 in Mach number was apparent in the flight/tunnel comparisons[6] of pressure distributions measured under supercritical flow conditions on the Super VC10. In neither example was the flow over the model wing of the class B type (premature rear separation) and hence, the conclusions regarding this scale effect even if genuine for the cases analysed, should not be extrapolated to future designs where the flow over the model may be of the class B type.

The aim behind the above remarks was to emphasize that the conclusions from this flight/tunnel drag comparison should be treated with reserve. Finally, three points of detail that should have been included in the text of the report :-

1. the tunnel interference corrections applied to incidence and drag are:

$$\Delta\alpha = -0.266\ C_L \quad \text{(degrees)}$$

$$\Delta C_D = -0.00465\ C_L^2$$

These are based on a comparison of the results for a model of a subsonic transport tested both in the tunnel with perforated walls and in the same tunnel with the holes taped over to give a closed working section,

2. the corrections applied to the quasi-level flight data to convert to $R = 1 \times 10^6$/ft amounted to less than ± 0.0002 in C_D except at $M = 0.82$, $C_L = 0.53$ and $M = 0.82$, $C_L = 0.137$ where the corrections were -0.00029 and $+0.00090$ respectively.

3. the drag increment of $\Delta C_D = 0.0005$ for the vortex generators, as measured in the tunnel tests did not vary significantly with Mach number until beyond (M_D +0.02). In flight, the drag increment due to the generators was only measured at low speeds ($\Delta C_D = 0.0003$) but it seems most unlikely that it would vary with Mach number sufficiently to have any influence on the flight/tunnel comparison of M_D.

REFERENCES

See main text

9th October 1973.

CONTENTS

FIGURES

1. INTRODUCTION

During the past few years considerable testing has been completed in the A.R.A. 9ft. x 8ft. transonic wind tunnel on models of various multi-engined jet transport and bomber aircraft. To help in assessing the reliability of these results and of the methods that can be used to convert them to flight Reynolds number, a series of special tests has been made to provide a detailed flight-tunnel comparison for some of these aircraft (Refs. 1 is typical) For these tests, the models are brought up to date relative to the full scale aircraft and, for the present tests on the Victor B. Mk.2, are fitted with many of the small details and excrescences that would not normally be represented.

Wind tunnel tests on the Victor model have been made in two stages: Phase I in which the model was mounted on a single sting support and in which tests were made with various elevator settings so as to obtain trimmed drags, and Phase II in which the model was mounted on twin stings from the wings to determine the corrections for the interference of the single sting used in Phase I.

Since the bulk of the flight data was only available in the form of curves and not tabulated data it has not been possible to present an analysis of that data in the same depth or style as in Ref. 1.
It has nevertheless been possible to fulfill the primary aim of this report which is to present a comparison of the corrected wind tunnel data (extrapolated to full scale Reynolds numbers) and the drag measured on the prototype aircraft XH 669. The drag comparisons cover a Mach number range from M = 0.70 to M = 0.90 for trimmed lift coefficients up to $C_L = 0.50$.

2. DESCRIPTION OF MODEL

The model used for the present series of wind tunnel tests was a 1/25 scale complete model of the Victor B.Mk.2. Figure 1 gives a general side and plan view of the model mounted on the single sting support. The size of the fuselage cut out necessary to accommodate the single sting was kept to a minimum, giving an external clearance of 0.40", and there was no distortion of the fuselage lines ahead of the cut-out.

The model wings (Fig. 2) were manufactured to take account of the wing aeroelastic distortions that would occur in full-scale cruising flight in the C_L range 0.35 to 0.45. The resultant model wing twist distribution was as follows:

STATION (fuselage centreline at -18)	INCIDENCE (to body centreline)	DIHEDRAL (40% chord)
		4.6°
212	4.275°	
		1.6°
330	2.017°	
		0.9°
702(tip)	-1.229°	

One particular area in which the model was non-representative of the full scale aircraft was in the nacelles where some cutting away of the nacelle underside ahead of the wing trailing edge was necessary to represent the full scale intake mass flow on the model.

For this series of tests the elevator angle was varied whilst the tailplane itself was set at a constant angle of - 52½ mins. relative to the fuselage centre line. This mode of operation was the same as the full scale aircraft.

For the single sting tests, vortex generators were fitted to the wing as shown in Fig.2. The size and spacing of these generators was scaled directly from the full scale aircraft with no allowance for the scale change in boundary layer thickness with Reynolds number.

Information regarding the detailed geometry and large excrescences present on the flight test aircraft was obtained from Messrs. Handley Page Ltd. and various items, some of which would not normally be represented in a wind tunnel test, were added to the model for the single sting tests. These extra items are marked in black in Fig. 1 and are also listed below:

1. Two small NACA intakes either side of the bomb aimers window, different on port and starboard. These were blanked off inside the duct.

2. Windscreen wiper housing on port side of windscreen.
3. Spar joint capping strips at two stations on upper and lower wing surfaces.
4. Artouste housing under starboard wing with intake retracted, Jet pipe represented.
5. Undercarriage door bulges.
6. Dorsal fin root intake, blanked off inside.
7. Small intakes on wing leading edge outboard of main intakes. These were blanked off inside the duct.
8. Nose probe with feel simulator intake.
9. Pitot static heads on both wing tips.
10. Elevator mass balance.
11. Small aerial on top of fuselage behind wing root.

Items not represented on the model, but present on the flight test aircraft, included vertical splitter plates in the main engine intakes, boundary layer bleed from inside the engine duct to the wing top surface, windscreen flats and control surface gaps (e.g. flaps, elevator). Apart from these items, the model still did not have the same surface finish as the aircraft e.g. no skin joints, spot welds, a few rivet heads etc. It is worth noting that it would be meaningless to represent these imperfections due to the"non-scale" effect of the boundary layer.

For the twin sting tests the model rear fuselage was split, at the position shown in Fig. 1, and connected to the fuselage centre section through a strain gauge balance. The complete model was supported by twin stings mounted on the wings. Tests were made with both a distorted rear fuselage (i.e. the single sting configuration) and with the correct rear fuselage. No excrescences or vortex generators were represented in these tests.

For both the single and twin sting tests boundary layer transition fixing bands of 0.0041" to 0.0049" diameter Ballotini set in Araldite were applied to the upper and lower surfaces of the wings and tailplane, starting at 5% chord and 1/8" wide. Bands were also applied to the fuselage, fin and bullet.

The balance used for both the single and twin sting tests was the No. 1 2¼" diameter six-component balance.

3. TEST PROCEDURE

Both the single and twin sting tests were made at nominal Mach numbers of M = 0.70, 0.76, 0.78, 0.80 (0.01) 0.92 at a stagnation pressure of 1 atmosphere. This gave an average Reynolds number range from $R_{\bar{c}_{gross}} = 3.24 \times 10^6$ at M = 0.70 to $R_{\bar{c}_{gross}} = 3.50 \times 10^6$ at M = 0.92 based on the mean geometric chord of the gross wing. In the main programme of single sting tests a total of five elevator angles were tested with the excrescences and vortex generators on the model. The angles (nominally $\eta = -5^\circ, -2^\circ, 0^\circ, +2^\circ$ and $+5^\circ$) were sufficient to cover trim conditions nearly the whole M ~ C_L range of interest. In a later series of tests the drag of some of the major excrescences was investigated by testing, at $\eta = 0^\circ$, firstly the complete model, then with the vortex generators removed, then with the vortex generators and wing excrescences removed and finally with the vortex generators and all excrescences removed. In the twin sting tests only $\eta = 0^\circ$ "vortex generators and all excrescences off" was tested.

Acenaphthene tests at M = 0.80, $\alpha = 2\frac{1}{2}^\circ$; M = 0.80, $\alpha = 4^\circ$ and M = 0.92, $\alpha = 1^\circ$ were made before the present series of drag tests. Transition was concluded from these tests to be fixed satisfactorily.

4. REDUCTION OF RESULTS

The wind tunnel results have been reduced to a non-dimensional form using the following data:

	Model Dimensions	Full Scale Dimensions
Gross Wing Area	4.155 ft.^{2}	2596.9 ft.^{2}
Gross Wing mean chord	0.866 ft.	21.65 ft.
Aspect Ratio	5.545	5.545

Pitching moments and trimmed drags are referred to a moment reference point situated at station 550" on the full scale aircraft.

Corrections to the results have been applied for sting and balance deflection under load, tunnel wall constraint on incidence and drag, tunnel flow pitch angularity, empty tunnel buoyancy, blockage (zero)*,

* There is evidence from other models that the blockage correction is zero up to about M = 0.86. Strictly speaking a negative correction is required beyond this Mach number - this correction might possibly be as large as $\Delta M = -0.003$ at M = 0.90.

blockage buoyancy, duct internal drag and transition band roughness drag. Corrections due to sting interference** on lift, drag and pitching moment have also been applied and the wind tunnel drags have been corrected to a constant $R_{\bar{c}_{gross}} = 3.4 \times 10^6$. The following table gives values of the above corrections at M = 0.70 and M = 0.90. More information regarding the derivation of the corrections can be obtained from Refs 1. All corrections have been applied according to the equation (e.g. for Drag Coefficients):-

$$C_{D_{corrected}} = C_{D_{measured}} + \Delta C_D$$

Quantity	Correction M=0.70	Correction M=0.90	Parameter
Pitch Angularity (relative to horizontal and not tunnel centreline)	-0.20°	-0.20°	Incidence (α)
Buoyancy	0	0	C_D
Blockage Buoyancy	0	-0.0002	C_D
Duct Internal Drag	-0.0008	-0.0008	C_D
Transition Band Roughness Drag	-0.00015	-0.0002	C_D
Reynolds number	-0.0001	+0.0001	C_D

5. DISCUSSION

5.1 Wind Tunnel Results

5.1.1 $C_L - \alpha$; $C_m - C_L$ Results

Figures 3(a-c) and 4(a-c) present the measured $C_L - \alpha$ and $C_m - C_L$ results for a selection of Mach numbers between M = 0.70 and M = 0.92 at each of the five elevator angles tested. In general the

** Although the twin sting configurations were only tested at one elevator angle ($\eta = 0^\circ$), experience with another high tail configuration suggests that, for the range of trimmed conditions considered here the use of sting corrections for $\eta = 0^\circ$ will introduce negligible errors in C_L and C_m and a likely maximum error of about 0.0001 in C_D.

effect of increasing elevator angle is as would be expected. The elevator power, $\frac{\partial C_m}{\partial \eta} = -0.010$/degree, is sensibly invariant with Mach number and incidence and the effect of increasing Mach number is to move the aerodynamic centre rearwards by about 9% $\bar{c}_{gross}$

5.1.2 Trimming

In fig. 5 is presented a comparison of the variation of elevator angle to trim over a range of trimmed C_L and Mach number as measured in the wind tunnel and in flight. It will be seen that the apparent wind tunnel-flight discrepancy is consistently about 1^o at M = 0.70, decreasing slightly up to about M = 0.80 and then increasing to about 2^o at high M i.e. the discrepancy is within the quoted flight data accuracy of $\pm 1^o$ up to about M = 0.80 but not at higher Mach numbers. Possible reasons for this include a C_{m_o} effect, perhaps due to a significant variation with M in the aeroelastic distortion of the wing in flight related to the aerodynamic centre movement, and also wind tunnel-flight differences in fuselage bending due to the tailplane loads.

5.1.3 Drag measurements and comparison with estimates

Dealing first with the method of drag estimation it should be noted that the estimates, as plotted in Fig.6, have been made for a clean model and do not take account of any possible interference effects. The estimates (which are presented in detail in Appendix A) have been made using the C_f - R curves of Ref.3 together with appropriate form factors derived from the Royal Aeronautical Society Wings and Bodies Data sheets. The charts of Ref.2 are based on the Prandtl - Schlichting expression for turbulent skin friction and in using them, one can take account of the actual model and assumed flight transition positions at tunnel and flight Reynolds numbers respectively. A sweep factor allowance has been included in the wing, tailplane and fin estimates. To the complete model estimates has been added an estimated allowance of 0.0003 in C_D at model scale and 0.0002 in C_D at full scale Reynolds numbers to account for the excrescences (items 1-11) mentioned in Section 2. From the excrescence drag investigation (see Section 3) drag increments of about $\Delta C_D = 0.0001$ and $\Delta C_D = 0.0003$ were measured at low Mach number for the wing excrescences and for the combined fuselage, tailplane and bullet excrescences respectively i.e. as far as experimental accuracy allows, the combined total increment supported the excrescence drag estimates.

In addition to this total of $\Delta C_D = 0.0004$ a further $\Delta C_D = 0.0005$ for the vortex generators was measured.*

In figs. 7(a-d) are presented the fully corrected untrimmed wind tunnel drags for each of the five elevator angles tested. These plots of C_D - M are corrected to a model Reynolds number of $R_{\bar{c}_{gross}} = 3.4 \times 10^6$.

For the lowest Mach number of the wind tunnel tests (M = 0.70) and at $C_L = 0$ the lowest measured wind tunnel C_D was $C_D = 0.0139$ at $\eta = +2^o$. If extrapolations to $C_L = 0$ (i.e. ignoring the non-linear $C_D \sim C_L^2$ region between about $C_L = 0$ and $C_L = 0.20$ - see Fig.8 where the derivation of the actual $C_{D_{trimmed}} \sim C_L^2$ curve at M = 0.70 is shown together with the linear extrapolation to $C_L = 0$) and to M = 0 (because an M = 0.70 measured drag is not strictly comparable with an incompressible flow drag estimate) then reductions of 0.0009 and 0.0002 respectively in the measured C_D lead to an M = 0, $C_L = 0$ wind tunnel $C_D = 0.0128$. This value compares with an estimate of $C_{D_{pr.}} = 0.0127$ which includes an allowance of $\Delta C_D = 0.0003$ for items 1-11 at model scale Reynolds numbers and of $\Delta C_D = 0.0005$ for the measured vortex drag increment. Reference 3 has shown that the method of wing profile drag estimation used gives estimates which are typically 5% high for the zero lift profile drag of two dimensional sections. Admittedly the outer wing section is thinner than any considered in Ref. 4 but if it is assumed that the method of estimation used in Appendix A still overestimates by 5% when used in conjunction with a sweep factor on this wing, then the final complete model estimate reduces to $C_{D_{pr.}} = 0.01235$.

---

* The wind tunnel measured value of $\Delta C_D = 0.0005$ compared with a low speed flight measured value of $\Delta C_D = 0.0003$. No flight measured figure is available for the other excrescences.

Before considering the flight data it should be noted that the use of the flight measured values of η_{trim} (i.e. instead of the wind tunnel values) would increase, at M = 0.70, the values of $C_{D_{trimmed}}$ by between about ΔC_D = 0.0003 and ΔC_D = 0.0005, dependent on C_L, with a slight reduction in ΔC_D at higher Mach number and would therefore tend to reduce the values of wind tunnel drag-rise Mach number at trimmed conditions by between about ΔM = 0.005 and ΔM = 0.010.

These comments clearly indicate a marked sensitivity to elevator angle. Two possible reasons for the apparent discrepancy between the wind tunnel and flight measured values of η_{trim} have already been mentioned in 5.1.2. If the difference is entirely due to fuselage bending then the use of tunnel angles to trim would be appropriate since tailplane load is the most significant factor. If the variation of the discrepancy with Mach number is due to variations in the aeroelastic distortion of the wing in flight related to the aerodynamic centre movement then the form of the variation of tailplane drag with Mach number is closely approximated by the use of the flight measured elevator angles to trim, but in this case the wing drag is different on the model and in flight. Almost certainly however the sole use of either set of measured values of elevator angles to trim throughout the whole M - C_L range would be incorrect.

5.2 Flight Results: Derivation and Correction of Flight Data

Using the prototype aircraft XH669 a total of twelve flight conditions were flown using the quasi-level technique*. These points covered two types of flight i.e. variable C_L at M = 0.819 and variable M at C_L = 0.35, together with two flight conditions at C_L = 0.443, M = 0.870 and at C_L = 0.115, M = 0.628. In addition to these quasi-level flights some additional information was collected during

---

* The quasi-level technique can best be described as follows:- with the engine power set for substantially level flight the aircraft is flown as near as possible at constant I.A.S. From the continuous trace records of the flight, values of $\frac{dH}{dt}$ and $\frac{dV}{dt}$ are determined and used to correct the flight data to straight and level flight conditions at constant I.A.S.

engineering tests on the prototype. From these engineering test results, which are less accurate than the quasi-level data (readings were taken less frequently and under less steady flight conditions), a carpet plot of $C_D - C_L$; M was derived by Handley Page Ltd. and is reproduced in Fig. 9. For each flight point, values of gross thrust and engine mass flow (and hence net thrust) have been estimated using flight pressure measurements and a Rolls Royce calibration curve. The calibration tests included measurements on one engine in the high altitude test bed plant. In the thrust calculations a ram pressure recovery factor = 0.92 was assumed in the intake, this value having been derived from wind tunnel tests. The flight points have all been corrected to a constant $R = 1 \times 10^6$/ft. (full scale) using a curve originally presented in Ref.4. This curve is reproduced in Fig.6 and is positioned to coincide with the A.R.A. curve at $R = 1 \times 10^6$/ft. Finally the flight data has been corrected to either constant C_L or constant Mach number. The effect of using the A.R.A. derived $C_{D_{pr.}}$ - R variation (instead of the Handley Page Ltd. variation) to convert the flight data to a constant $R = 1 \times 10^6$/ft. would be most marked for the M = 0.819 quasi-level data where the Reynolds number range is between $R = 0.75 \times 10^6$/ft. ($C_L = 0.531$) and $R = 2.64 \times 10^6$/ft. ($C_L = 0.137$). At the high Reynolds number condition the effect of using the A.R.A. curve would be to increase C_D (flight) by about $\Delta C_D = 0.0005$. This is however an extreme condition and over most of the range of the quasi-level data (the only data for which the Reynolds numbers are known at A.R.A.) the correction would be less than about $\Delta C_D = \pm 0.0001$. The correction to constant M or C_L was made by Handley Page Ltd. using a fairing technique which only used the data itself and did not rely, for example, on $C_D - C_L$ or C_D - M trends as measured in any wind tunnel test.

5.3 Wind Tunnel - Flight Comparison

In Figs. 10a,b are presented wind tunnel - quasi level flight trimmed drag comparisons, $C_{D_{trimmed}} - C_L$ and $C_{D_{trimmed}}$ - M, for the two major flight conditions together with, in Fig. 11, a comparison of wind tunnel and engineering flight trimmed drags, $C_{D_{trimmed}}$ - M, for a range of C_L's. Care should be taken in interpreting these figures due to the different $C_{D_{trimmed}}$ scales. (A scale of

ΔC_D = 0.005 per 2 cms. is used in Fig. 11 which is a reproduction, at approximately the same scale, of the original Handley Page Ltd. graph. Figures 10a,b use a more sensitive scale of ΔC_D = 0.002 per 2 cms. to present the quasi-level flight data tabulated in Ref.5). It should be noted that the flight data curves presented in Figs. 10a,b have been drawn taking into account both the engineering test flight data and the quasi-level data. This use of both types of flight data to derive a mean line is the reason for the apparent lack of fit of the quasi-level data in Figs. 10a,b.

The wind tunnel results have been extrapolated to $R_{\bar{c}_{gross}} = 21.7 \times 10^6$ ($R = 1 \times 10^6$/ft.) using the estimated $C_{D_{pr.}} - R_{\bar{c}_{gross}}$ variation of Fig.6. The wind tunnel results have been obtained from crossplots of $C_D - \eta$ at the tunnel values of η_{trim} in Fig.5. Values of C_D at η_{trim} outside the range tested in the wind tunnel have been obtained by extrapolation. Before dealing with the differences between the extrapolated wind tunnel and measured flight drags it is useful to briefly reconsider the differences between wind tunnel and flight as mentioned on page 3. These were splitter plates, boundary layer bleeds, windscreen flats, control surface gaps, skin joints, rivet groups etc. Besides these differences it is probable that there are some additional small excrescences e.g. ice detectors, dumps (for both gases and liquids), actuators (ailerons and elevators) etc. on the aircraft. It should be stated here that, unlike Ref.1, no allowance has been made in Figs. 10 and 11 for the items not represented on the model.

If we now compare the extrapolated wind tunnel and flight trimmed drags (using elevator angles to trim for tunnel) in Figs. 10 and 11 then the wind tunnel underestimation, by generally up to about ΔC_D = 0.0008 for $C_L \leq 0.40$ and $M \leq 0.80$, could be wholly, or at least partially, accounted for by the model-full scale aircraft differences mentioned above and/or by the use of the flight derived values of η_{trim} - section 5.1.3. (this would effectively raise the level of the extrapolated wind tunnel curves by between ΔC_D = 0.0003 and ΔC_D = 0.0005 dependent on C_L). For $C_L > 0.40$ however the wind tunnel underestimate rapidly changes to become, at C_L = 0.50; M = 0.70, an overestimate of about ΔC_D = 0.0015. Although Fig.9 shows the full scale drag as being independent of M for M < 0.76 it is not known how much evidence there is for this, it is certainly not true of the wind tunnel data at C_L = 0.50

and only approximately correct for the range $C_L = 0.35$ to $C_L = 0.45$ inclusive. It should be noted here however that it is not known how well the extremes of the carpet are supported by the experimental evidence.

If we consider now several aspects of the comparison then we can see that, subject to the above comments on the flight data:-

1) at low Mach number the flight data tends to have a more linear $C_D - C_L^2$ relationship than the wind tunnel data (the flight data becomes non-linear for $C_L > 0.45$ compared with $C_L > 0.30$ for the wind tunnel data). Over the linear part of the range the flight and wind tunnel values of induced drag factor are in good agreement,

2) the Mach number for the steep drag-rise is higher in the tunnel than in flight by an amount that varies between about $\Delta M = 0.005$ and $\Delta M = 0.015$ ($C_L = 0.10$ to $C_L = 0.35$) and that increases rapidly at the highest C_L of the comparison. It should be noted that the apparent discrepancy in drag-divergence Mach number M_D is observed near $M = 0.85$ i.e. at a Mach number where evidence from tests on other models in the A.R.A. tunnel shows that the zero blockage correction used here, should be valid. Even at $M = 0.90$, it is thought that the blockage correction (still taken as zero) could be only about $- 0.003$ in M. Hence if a discrepancy in drag-rise Mach number is accepted as a genuine conclusion from the analysis despite the doubts related to the elevator angles to trim and possible aeroelastic effects, it seems that the more likely source is scale effect rather than tunnel wall interference. A possible mechanism for scale effect could be that in the tunnel, the boundary layer at the wing trailing edge is thicker than in flight; this leads to a poorer pressure recovery and perhaps, a further forward shock position e.g. relative to the crest and hence, a delayed increase in wave drag with Mach number. In a Class A flow situation (no incipient rear separation) - and there is no doubt that the present tests would be in this category - this could dominate the scale effect on drag-rise Mach number. The flight-tunnel comparisons (Ref. 5) of wing pressure distributions on the Super VC.10 lend support to these remarks concerning relative shock positions in tunnel and flight. Use of the flight derived values of η_{trim} to derive the trimmed wind tunnel drags would tend to reduce the values of wind tunnel drag-rise Mach number by between $\Delta M = 0.005$ and $\Delta M = 0.010$ and would generally give reasonable agreement for $C_L \leq 0.35$.

6. CONCLUSIONS

In this report the results of a wind tunnel-flight comparison for the Victor B.Mk.2 have been analysed.

At wind tunnel Reynolds numbers reasonable agreement has been shown to exist between the measured wind tunnel drag and the profile drag estimated by a simple method. The measured and estimated drag penalty of the full scale excrescences represented on the model has also been shown to be in reasonable agreement.

Although it is difficult to draw firm conclusions at conditions other than those studied during the quasi-level flight tests i.e. variable Mach number at $C_L = 0.35$ and variable C_L at $M = 0.819$ several conclusions can be drawn from the wind tunnel - flight comparison:-

1) A comparison of the wind tunnel and flight derived values of η_{trim} at various M and C_L conditions indicate discrepancies of the order of $1^o - 2^o$ although quite plausible reasons as to why this difference could be genuine are suggested.

Both the drag levels and the drag rise Mach number are sensitive to the values of η_{trim} used. In the following conclusions the effect of using either set of values are described but it should be noted that the use of either one set or the other throughout the whole $M - C_L$ range is unlikely to be correct.

2) An extrapolation of the wind tunnel data to flight Reynolds numbers, without an allowance for excrescences not represented on the model, tends to underestimate the flight data by about $\Delta C_D = 0.0008$ for $C_L \leqslant 0.40$ and up to about $M = 0.80$ and thereafter, for increasing C_L, the underestimate rapidly changes to an overestimate. At C_L's up to $C_L = 0.40$ it is suggested that the inclusion of a drag allowance for model-full scale aircraft differences, possibly also with the use of the flight derived values of η_{trim}, could produce a very good comparison for Mach numbers up to just below the start of the steep drag rise. For high C_L's it is not known how well the extremes of the carpet are supported by the experimental evidence.

3) For the linear part of the $C_D - C_L^2$ curves the wind tunnel and flight data tend to have very similar values of lift induced drag factor at low Mach number, with the wind tunnel data tending to become non-linear for $C_L > 0.30$ compared with $C_L > 0.45$ for the flight data.

4) The comparison of the drag-rise Mach numbers (using the wind tunnel derived values of η_{trim}) shows the disagreement to vary between

0.005 and 0.015 in Mach number for $C_L \leq 0.35$ and to increase rapidly at high C_L - the wind tunnel having the higher values. The use of the flight derived values of η_{trim} reduces the difference significantly and would generally give good agreement for $C_L \leq 0.35$.

5) It seems fair to conclude that the results suggest that for a wing where the flow is of Class A (no incipient rear separation), there may be an adverse scale effect on the drag - divergence Mach number. In the present case, this could have been of the order of 0.01 (higher M_D in the tunnel) but the precise magnitude and even the existence of this effect is uncertain because of some doubts about the flight data and the possible aeroelastic effects.

NOTATION

A	Aspect Ratio
C_D	Drag Coefficient
$C_{D_{trim}}$	Trimmed drag coefficient
$C_{D_{pr.}}$	Profile drag coefficient
C_f	Skin friction coefficient
C_L	Overall lift coefficient
C_m	Pitching moment coefficient
$\bar{c}_{gross}$	Gross wing mean chord (ft).
H	Altitude (ft.)
k	Induced drag factor ($k = \dfrac{\Delta C_D . \pi . A}{\Delta C_L^{\ 2}}$
M	Freestream Mach number
M_D	Drag-divergence Mach number
R	Reynolds number
$R_{\bar{c}_{gross}}$	Reynolds number based on $\bar{c}_{gross}$
t	Time
V	Velocity
α	Fuselage incidence (degrees)
η	Elevator angle (degrees)
η_{trim}	Elevator angle at trimmed condition (degrees)
ΔC_D	Increment in C_D
ΔC_L	Increment in C_L
ΔM	Increment in M
$\dfrac{dH}{dt}$	Rate of change of altitude with time
$\dfrac{dV}{dt}$	Rate of change of velocity with time

REFERENCES

No.	Author(s)	Title, etc.
1	J. I. Simper and P. G. Hutton	Results of a series of Wind Tunnel Model Breakdown Tests on the Trident 1 aircraft and a comparison with Drag Estimates and Full Scale Flight Data. ARC CP No.1170. March, 1970.
2	D. W. Clutter	Charts for Determining the Skin Friction Coefficients on Smooth and on Rough Flat Plates at Mach numbers up to 5.0 with and without Heat transfer. Douglas Report ES 29074. April, 1959.
3	H. H. Pearcey and J. Osborne	On Estimating Two-Dimensional Section Drag. A.R.C.27 872. March, 1966.
4	J. K. Robinson	Victor B. Mk.II. XH 669. Summary of Performance Measurements. HP/AERO/5008. 9th November, 1961.
5	Miss G. C. Browne, T. E. B. Batemann, M. Pavitt and A. B. Haines	A comparison of wing pressure distributions measured in flight and on a wind tunnel model of the Super VC 10. ARC R & M 3707. November, 1971.

APPENDIX A

PROFILE DRAG ESTIMATES FOR THE VICTOR B.Mk.2

The principal aim of this report has been to compare the measured wind tunnel model drag and the full scale aircraft drag. An essential step in this comparison is the need to be able to accurately predict how the aircraft profile drag will vary between the model and full scale Reynolds number range. To this end estimates of the model and full scale profile drag have been prepared and, for the sake of completeness, are presented in the following pages together with explanatory notes and references where applicable. In general the estimates are quite self explanatory and follow current practice. Where different interpretations of how certain effects should be considered, e.g., definition of fuselage fineness ratio, the definition of source of data is clearly stated. In addition to the tables and notes a somewhat idealised drawing of the aircraft has been included to indicate the assumed intersection lines of various components.

TABLE A1
PROFILE DRAG OF FUSELAGE

	MODEL SCALE			FULL SCALE			
Reference Dimensions							
Gross Wing Area (ft^2)	4 155			2596 9			
Gross Wing Mean Chord $\bar{c}$ (ft)	0 866			21 65			
Lengths (ft) (1)							
Forebody (2)	0·967			24 167			
Parallel Section (3)	1 398			34 959			
Afterbody (4)	1·715			42 874			
Total	4 080			102 0			
Maximum Body Equiv Diameter (ft) (5)	0 429			10 732			
Effective Fineness Ratio (6)	0 121			0 121			
Wetted Area (ft^2) (7)	4 034			2521 2			
R per foot ($\times 10^{-6}$)	2·309	3 464	4 619	0 462	0 924	1 154	3 002
$R_{\bar{c}}$ gross ($\times 10^{-6}$)	2 0	3 0	4 0	10 0	20 0	25 0	65 0
R Body Length ($\times 10^{-6}$)	9·4	14·1	18 8	47 1	94 3	117 7	306 2
% Transition Position (8)	1·5	1 5	1 5	0	0	0	0
Form Factor (λ) (9)	1 081	1 081	1 081	1 083	1 083	1 083	1 083
Flat Plate C_f (10)	0 00302	0 00282	0 00270	0 00238	0 00215	0·00208	0 00166
λ x Flat Plate C_f	0·00326	0 00305	0 00292	0·00258	0 00233	0 00225	0 00180
D/q (ft^2)	0·01315	0 01230	0 01178	6 5047	5 8744	5 6727	4 5382
C_D	0·00316	0 00296	0 00284	0 00250	0 00226	0 00218	0 00175

TABLE A2
PROFILE DRAG OF WING

	MODEL SCALE			FULL SCALE			
Reference Dimensions							
Gross Wing Area (ft^2)	4 155			2596 · 9			
Gross Wing Mean Chord $\bar{c}$ (ft)	0·866			21 · 65			
Streamwise Local Chords (ft)(1)(11)							
Root (STN 42)(12)	1 633			40 83			
Trailing Edge Kink (STN 154)	1 148			28 70			
Leading Edge Kink 1 (STN 212)	0 990			24 74			
Leading Edge Kink 2 (STN 330)	0 789			19 73			
Tip (STN. 702)(13)	0 396			9 89			
% Thickness Chord Ratio(14)							
STN. 42	14 40			14 40			
STN 154	13 33			13 33			
STN 212	9 98			9 98			
STN 330	8 00			8 00			
STN 702	6 00			6 00			
Wetted Area (ft^2)(15)	7 244			4527 5			
R per foot ($\times 10^{-6}$)	2·309	3 464	4 619	0 462	0 924	1 154	3 002
$R_{\bar{c}}$ gross ($\times 10^{-6}$)	2 0	3 0	4 0	10 0	20 0	25 0	65 0
% Transition Position(8)	5·0	5 0	5 0	0	0	0	0
λ Unswept(16)							
STN 42	1 50	1 50	1 50	1 52	1 52	1 52	1 52
STN 154	1 47	1·47	1 47	1 48	1 48	1 48	1 48
STN 212	1 35	1 35	1 35	1 36	1 36	1 36	1 36
STN 330	1 28	1·28	1 28	1 29	1 29	1 29	1 29
STN 702	1·21	1 21	1 21	1 22	1·22	1 22	1 22
50 % Chord Sweep (degrees)(17)							
STN 42 to STN 154	33 0	33 0	33 0	33 0	33 0	33 0	33 0
STN 154 to STN 212	41 4	41·4	41 4	41 4	41 4	41 4	41 4
STN 212 to STN 330	35 8	35 8	35 8	35 8	35 8	35·8	35 8
STN 330 to STN 702	28 2	28 2	28 2	28 2	28 2	28 2	28 2
λ Swept(18) (using inb'd(19)/outb'd(20) sweep)							
STN 42	– /1 352	– /1 352	– /1 352	– /1 366	– /1 366	– /1 366	– /1 366
STN. 154	1 331/1 265	1·331/1 265	1 331/1 265	1 338/1 270	1 338/1 270	1 338/1 270	1 338/1 270
STN 212	1 197/1 231	1 197/1 231	1 197/1 231	1 203/1 237	1 203/1 237	1 203/1 237	1 203/1 237
STN 330	1 184/1 218	1 184/1 218	1 184/1 218	1 191/1 226	1·191/1 226	1 191/1 226	1 191/1 226
STN 702	1 163/ –	1·163/ –	1 163/ –	1 172/ –	1 172/ –	1 172/ –	1 172/ –

Continued on next page

TABLE A2
PROFILE DRAG OF WING

	MODEL SCALE			FULL SCALE			
Reference Dimensions							
Gross Wing Area (ft^2)	4·155			2596·9			
Gross Wing Mean Chord $\bar{c}$ (ft.)	0·866			21 65			
R per foot ($\times 10^{-6}$)	2 309	3 464	4 619	0 462	0 924	1 154	3· 002
$R_{\bar{c}}$ gross ($\times 10^{-6}$)	2· 0	3 0	4 0	10 0	20 0	25 0	65 0
Flat Plate C_f (10)							
STN. 42	0 00338	0 00316	0 00303	0 00276	0 00246	0 00239	0 00206
STN 154	0·00362	0 00336	0 00320	0 00292	0 00261	0·00252	0 00219
STN 212	0·00371	0 00346	0 00328	0 00296	0 00266	0 00259	0 00223
STN 330	0 00388	0 00360	0 00344	0 00308	0·00274	0 00267	0 00232
STN 702	0 00444	0 00408	0 00388	0 00328	0 00306	0 00297	0 00257
Total D/q (ft^2) (21)	0 03399	0 03154	0 03010	16 956	15 199	14 791	12 803
C_D	0 00818	0 00759	0 00724	0 00653	0 00585	0 00570	0 00493

TABLE A3
PROFILE DRAG OF FIN

	MODEL SCALE			FULL SCALE			
Reference Dimensions							
Gross Wing Area (ft^2)	4 155			2596 9			
Gross Wing Mean Chord $\bar{c}$ (ft)	0·866			21 65			
Fin Mean Chord (ft)	0 456			11 40			
Wetted Area (ft^2)[22]	0 412			257·6			
% Thickness Chord Ratio	10·75			10 75			
R per foot ($\times 10^{-6}$)	2 309	3 464	4 619	0 462	0 924	1 154	3 002
$R_{\bar{c}}$ gross ($\times 10^{-6}$)	2 0	3 0	4 0	10 0	20 0	25 0	65 0
R Fin Mean Chord ($\times 10^{-6}$)	1 053	1 580	2 106	5 27	10 53	13 16	34 22
% Transition Position[8]	5·0	5 0	5 0	0	0	0	0
λ Unswept[16]	1 380	1 380	1 380	1 390	1 390	1 390	1·390
50% Chord Sweep (degrees)	44·4	44·4	44 4	44 4	44 4	44 4	44 4
λ Swept[18]	1 194	1 194	1·194	1·199	1 199	1 199	1 199
Flat Plate C_f[10]	0 00432	0 00397	0 00376	0 00336	0 00302	0·00291	0 00250
λ Swept x Flat Plate C_f	0 00516	0 00474	0 00449	0 00403	0 00362	0 00349	0·00300
D/q (ft^2)	0 00213	0 00195	0 00185	1 0381	0 9325	0 8990	0 7728
C_D	0 00051	0 00047	0 00045	0 00040	0 00036	0 00035	0 00030

TABLE A4
PROFILE DRAG OF TAILPLANE AND BULLET

	MODEL SCALE			FULL SCALE			
Reference Dimensions							
Gross Wing Area (ft^2)	4 155			2596 9			
Gross Wing Mean Chord $\bar{c}$ (ft)	0 866			21 65			
Lengths (ft)[1]							
Tailplane Root[23]	0 619			15 47			
Tailplane Kink	0 279			6 96			
Tailplane Tip[13]	0 135			3 38			
Tailplane Mean Chord	0 307			7 67			
Bullet	0 795			19 88			
Bullet Max Equiv Diameter[5]	0 068			1 71			
% Thickness Chord Ratio							
Tailplane Root	7 82			7 82			
Tailplane Kink	8 70			8 70			
Tailplane Tip	8 70			8 70			
(d/l) Bullet	0 086			0 086			
Wetted Areas (ft^2)							
Tailplane[15]	0 802			501 0			
Bullet[24]	0 106			66 1			
R per foot ($\times 10^{-6}$)	2 309	3 464	4 619	0 462	0 924	1 154	3 002
$R_{\bar{c}}$ gross ($\times 10^{-6}$)	2 0	3 0	4 0	10 0	20 0	25 0	65 0
$R_{\bar{c}}$ Tailplane ($\times 10^{-6}$)	0 708	1 062	1 417	3 54	7 09	8 85	23 02
R_{length} Bullet ($\times 10^{-6}$)	1 84	2 75	3 67	9 18	18 37	22 94	59 68
% Transition Position, Tailplane[8]	5·0	5 0	5 0	0	0	0	0
% Transition Position Bullet[8]	1 5	1 5	1 5	0	0	0	0
λ Unswept Tailplane[25] (Root/Kink)	1·250/1 280	1 250/1 280	1 250/1 280	1 260/1 290	1 260/1 290	1 260/1 290	1 260/1 290
Tailplane 50% Chord Sweep (degrees)[26]							
Inner Panel	48 5	48 5	48 5	48 5	48 5	48 5	48 5
Outer Panel	37 7	37 7	37 7	37 7	37 7	37 7	37 7
λ Swept[18]							
Root	1 110	1 110	1 110	1 114	1 114	1 114	1 114
Kink[19] (inb'd sweep)	1 123	1 123	1 123	1 128	1 128	1 128	1 128
Kink[20] (outb'd sweep)	1 175	1 175	1 175	1 182	1 182	1 182	1 182
Tip	1 175	1 175	1 175	1 182	1 182	1 182	1 182
λ Bullet[9]	1 041	1 041	1 041	1 046	1 046	1 046	1 046
Flat Plate C_f[10]							
Tailplane Root	0 00408	0 00375	0 00358	0 00320	0 00286	0 00276	0 00237
Tailplane Kink	0 00475	0 00436	0 00415	0 00364	0 00324	0 00312	0 00269
Tailplane Tip	0 00565	0·00515	0 00480	0 00415	0 00368	0 00354	0 00302
Bullet	0 00390	0·00368	0 00352	0 00306	0 00275	0 00267	0 00231
D/q (ft^2)[21]							
Tailplane	0 00484	0 00444	0 00423	1 9342	1 7226	1 6607	1 4266
Bullet	0 00043	0 00041	0 00039	0 2116	0 1901	0 1846	0 1597
C_D Tailplane	0 00116	0·00107	0 00102	0 00074	0·00067	0 00064	0 00055
C_D Bullet	0.00010	0·00010	0·00009	0 00008	0 00007	0 00007	0 00006

TABLE A5
SUMMARY OF VICTOR B Mk2 PROFILE DRAG ESTIMATES

	MODEL SCALE			FULL SCALE			
R per foot ($\times 10^{-6}$)	2 309	3·464	4·619	0 462	0·924	1 154	3 002
$R_{\bar{c}}$ gross ($\times 10^{-6}$)	2 0	3 0	4 0	10 0	20 0	25·0	65 0
C_D Fuselage	0 00316	0 00296	0 00284	0·00250	0·00226	0 00218	0·00175
C_D Wing	0 00818	0 00759	0·00729	0 00653	0·00585	0 00570	0 00493
C_D Fin	0 00051	0 00047	0·00045	0·00040	0 00036	0·00035	0 00030
C_D Tailplane	0·00116	0 00107	0·00102	0·00074	0·00067	0·00064	0·00055
C_D Bullet	0 00010	0 00010	0 00009	0·00008	0 00007	0 00007	0·00006
C_D Complete Aircraft	0 01311	0 01219	0 01169	0·01025	0 00921	0·00894	0 00759

NOTES ON TABLES A1 - A4

The following brief notes are intended to provide additional information on the method, or source of data, used in the foregoing tables.

The annotated comments and references etc. refer to the numbers in the tables.

(1) The lengths in these tables are projected lengths along the horizontal fuselage datum as opposed to lengths measured along the surface of the body/section.

(2) The forebody is defined as the portion of fuselage extending from the nose of the body to the position of the maximum cross-sectional area i.e. the length of fuselage having a forward facing projected area.

(3) Although the length of the parallel section is not used in the estimates it should be noted that it is greater than (2 x Maximum Body Equivalent Diameter).

(4) The afterbody length is defined as the combined length of fuselage extending from the position of the maximum cross-sectional area to the start of the parallel section and from the end of the parallel section to the rear of the fuselage i.e. the overall length of fuselage with a rearward facing projected area.

(5) This is defined as:

$$\text{M.E.D.} = \sqrt{(\text{Max.C.S.A.})\ \frac{4}{\pi}}$$

(6) This is defined as:

$$\text{E.F.R.} = \frac{\text{M.E.D.}}{\text{length (forebody + afterbody)}+(2\text{xM.E.D.})}$$

(7) For the complete aircraft configuration the fuselage wetted area (in terms of full scale figures) is derived as follows:-

Forebody wetted area	=	607.6ft.^{2}	
Parallel section wetted area	=	1098.3ft.^{2}	
Afterbody wetted area (ahead of parallel)	=		370.7ft.^{2}
Afterbody wetted area (aft of parallel)	=		681.4ft.^{2}

Total Afterbody wetted area	= 1052.1ft.^{2}	
Area of two wing roots	= 313.6ft.^{2}	(subtracted)
Area of one fin root	= 11.5ft.^{2}	(subtracted)
Wing area inboard of STN.42	= 88.3ft.^{2}	(added)

Considering all these components then we have the total net fuselage wetted area = 2521.2ft.^{2}

The wetted areas themselves were obtained by graphically integrating the component periphery over its axial length.

(8) Each component of the full scale aircraft has been assumed to have leading edge transition. For the model transition has been assumed to take place at the start of the roughness band on each component surface.

(9) Obtained from an interpolation of R.Ae.S. Data sheets Bodies 02.04.01 and 02.04.02 (2nd Issue, January 1947).

(10) Obtained from an interpolation of M = 0, $C_f \sim R_\ell$ curves of Douglas Report No. ES.29074 (April 1959).

(11) All quoted wing spanwise station numbers are with reference to a fuselage centreline at STN.-18.

(12) The wing root chord is defined as being in the vertical plane of the fuselage side i.e. 60" full scale from the fuselage centreline.

(13) The tip chord has been defined as the streamwise chord length, at the tip station, of the lines projected along the wing/tailplane leading and trailing edges.

(14) Although only five streamwise thickness-chord ratios are presented the wing integration of (21) used data for a total of 10 stations.

(15) The wing/tailplane wetted area is defined as (4xplan area bounded by the wing/tailplane root chord, the wing/tailplane leading and trailing edges and the rounded tip) minus, in the case of the tailplane, the tailplane lower surface area covered by the bullet.

(16) Obtained from R.Ae.S. Data sheets Wings 02.04.03(b) (April 1953).

(17) For the purpose of establishing the 50% chord sweep angle the wing has been divided into the four panels as indicated.

(18) The definition of the swept form factor (λ_{swept}) used in these estimates is:

$$\lambda_{swept} = (\lambda_{unswept} - 1) \cos^2 \Lambda_{0.5c} + 1$$

where $\Lambda_{0.5c}$ is the angle of sweepback at 0.5c.

(19) (20) Although there is no discontinuity in the variation of streamwise t/c across adjacent wing panels there is a discontinuity in the $\Lambda_{0.5c}$ and hence the reason for presenting two values of λ_{swept} at the kink. (19) uses the inboard panel sweep angle and (20) uses the outboard panel sweep angle.

(21) Total (D/q) is obtained from an integration of the product of the local chord, local skin friction coefficient and the local swept form factor i.e.

$$\text{Total } (D/q) = 4 \int_{\text{wing root}}^{\text{wing tip}} (C_f \times c \times \lambda_{swept})_{local} \; d(\text{span})$$

(22) The fin wetted area is defined as (2 × side view area bounded by the fuselage surface, the fin leading and rudder trailing edges and the bullet lower surface).

(23) The tailplane root chord is defined as being in the vertical plane of the fuselage centreline i.e. STN. - 18.

(24) The bullet wetted area does not include any area covered by the fin or tailplane.

(25) Obtained from R.Ae.S. Data sheets Wings 02.04.03(a) (April 1953).

(26) The spanwise extent of the inner panel is defined as being from the tailplane root to the streamwise chord through the leading edge kink and the outer panel being from the streamwise chord through the leading edge kink to the tip station.

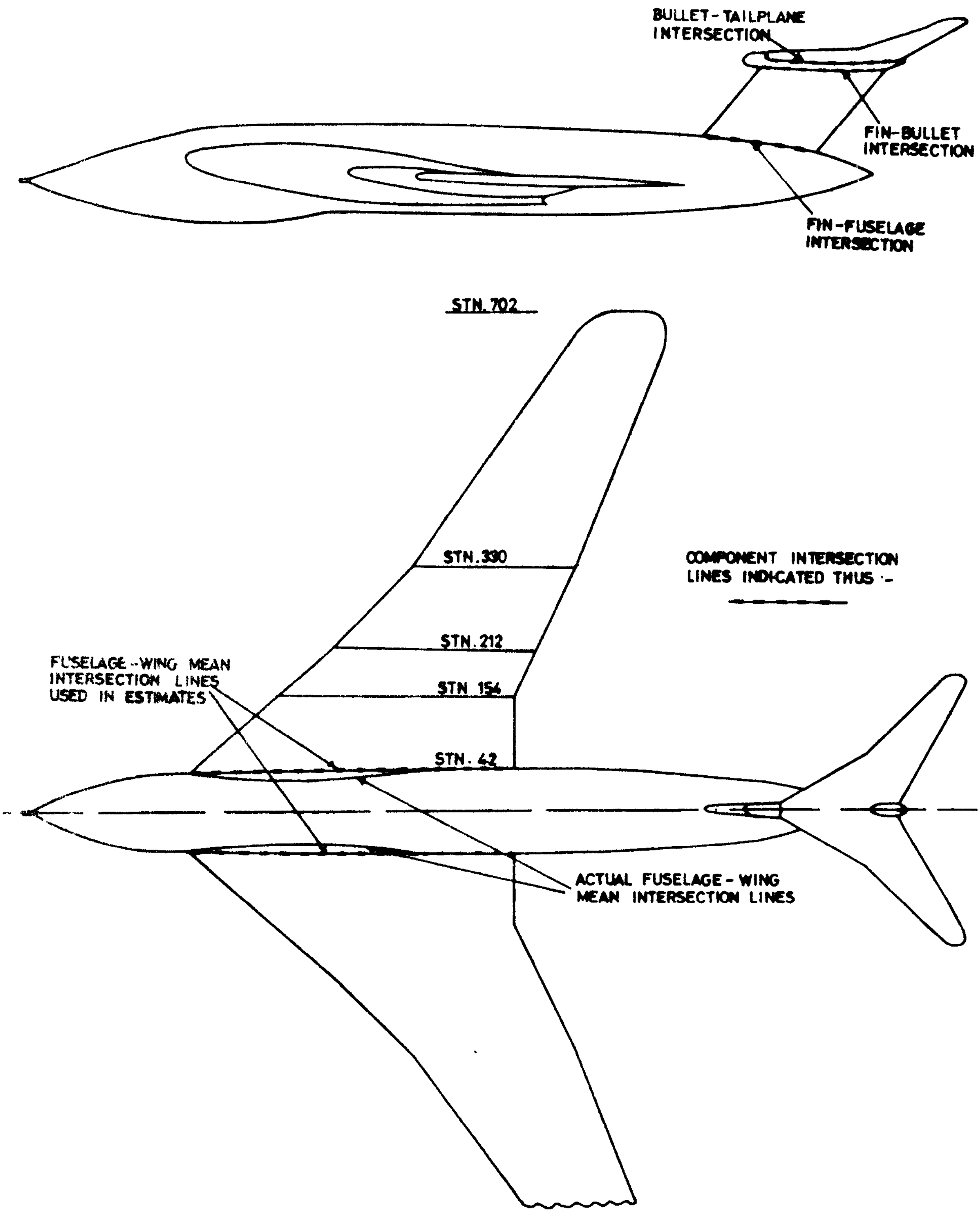

FIG. A1. INTERSECTION LINES FOR VICTOR B.Mk.2 MODEL.

FIG. 1

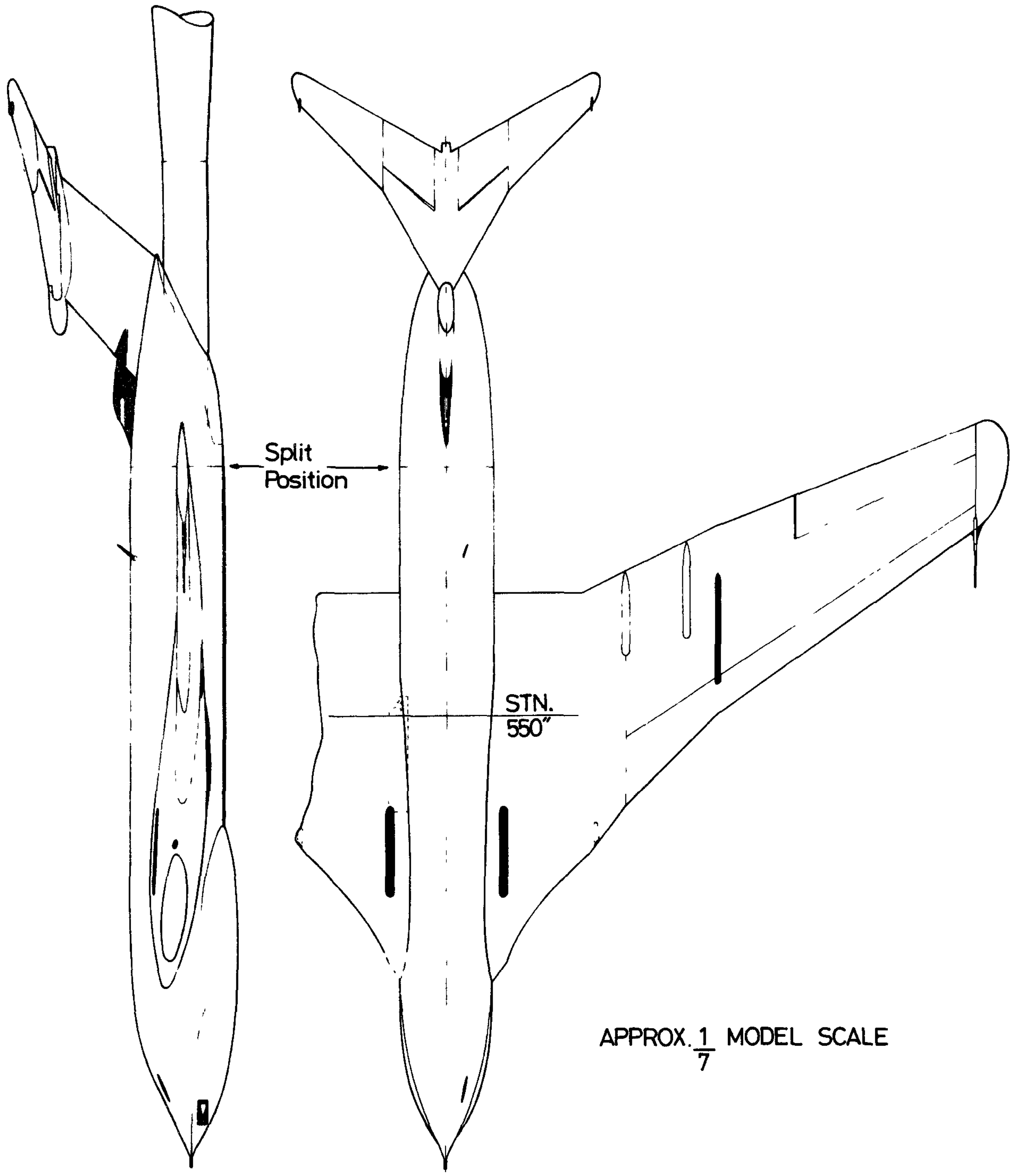

FIG. 1 DRAWING OF MODEL

FIG. 2.

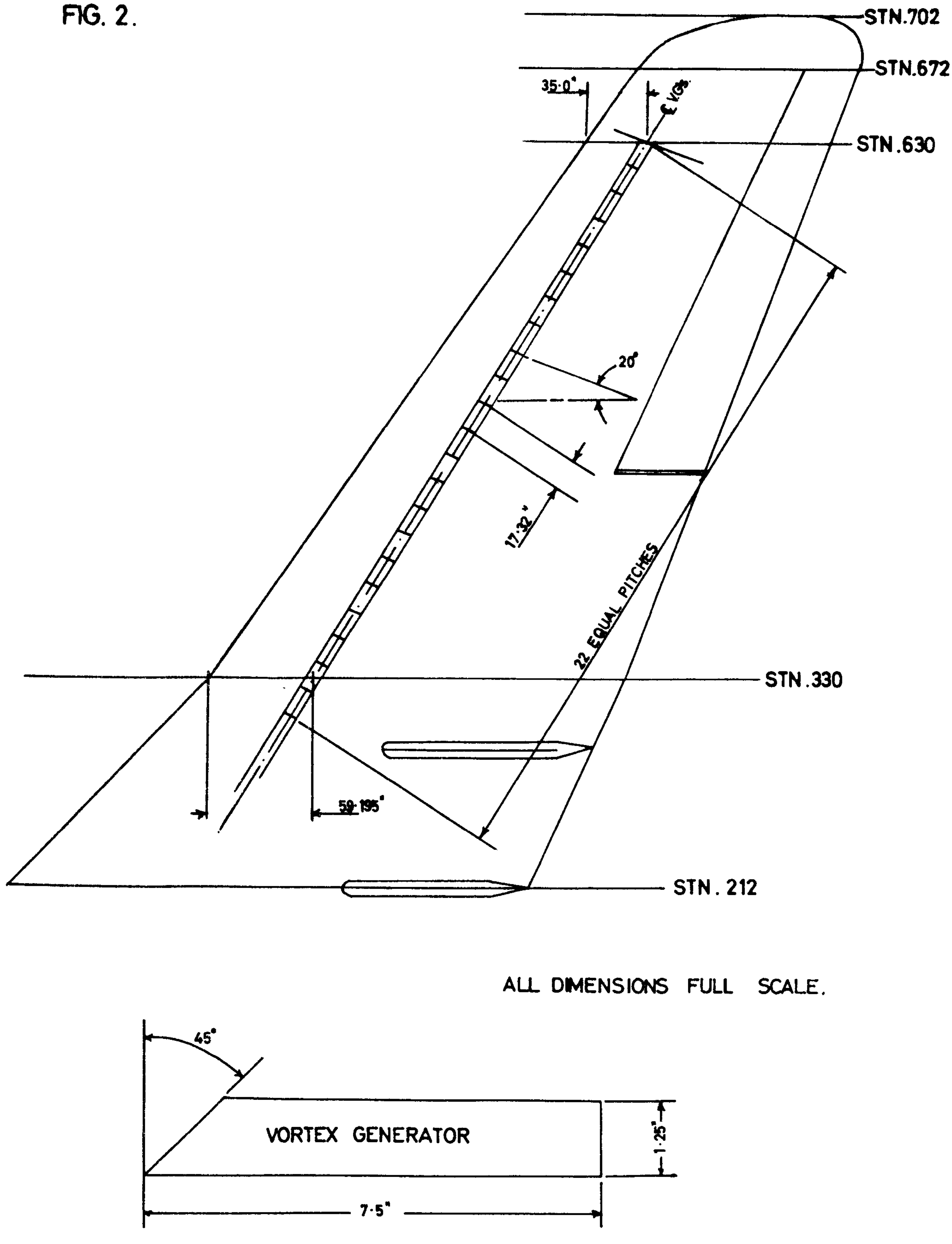

FIG.2 VORTEX GENERATOR CONFIGURATION

FIG. 3a. $C_L \sim \alpha$.

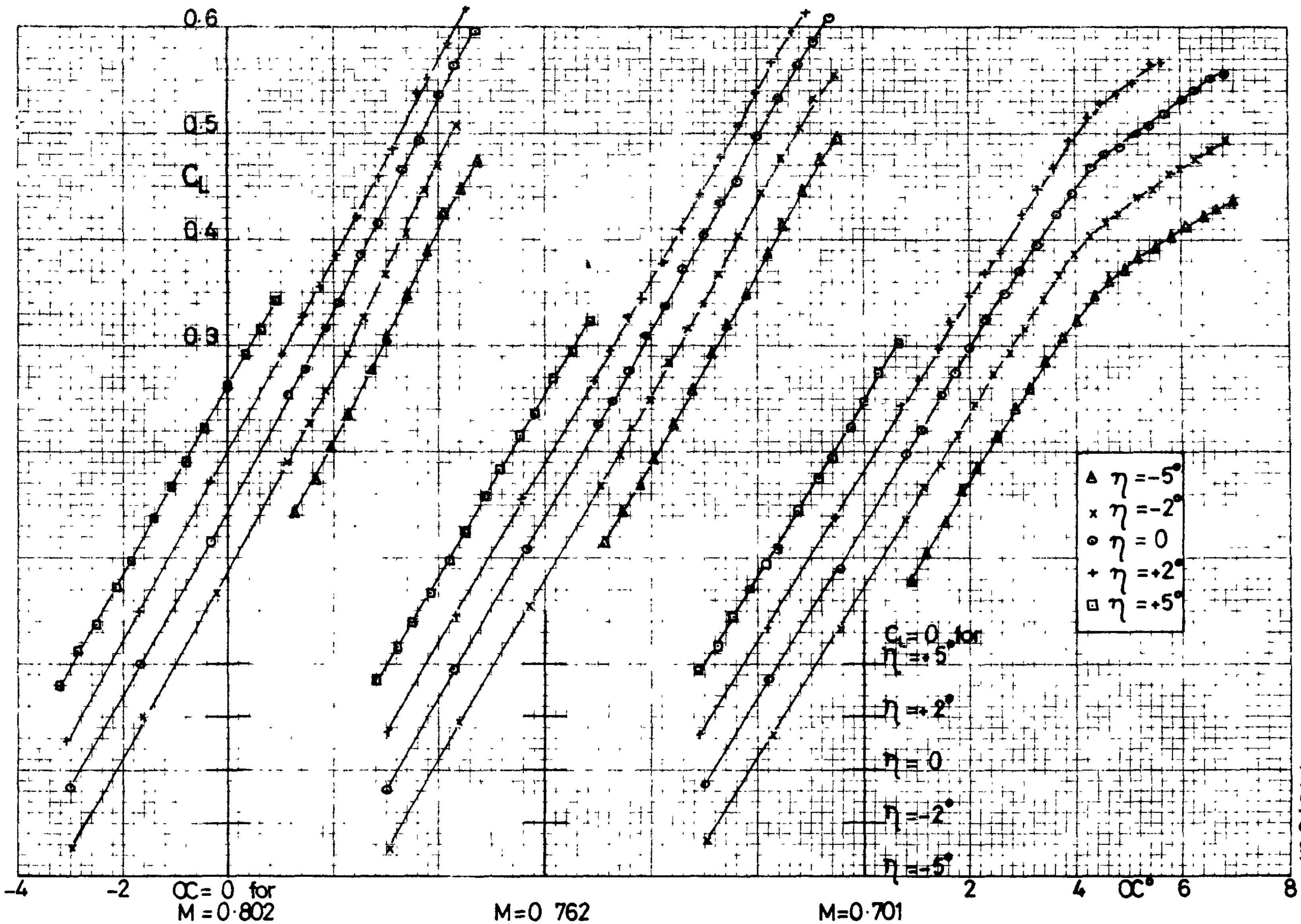

FIG. 3a.

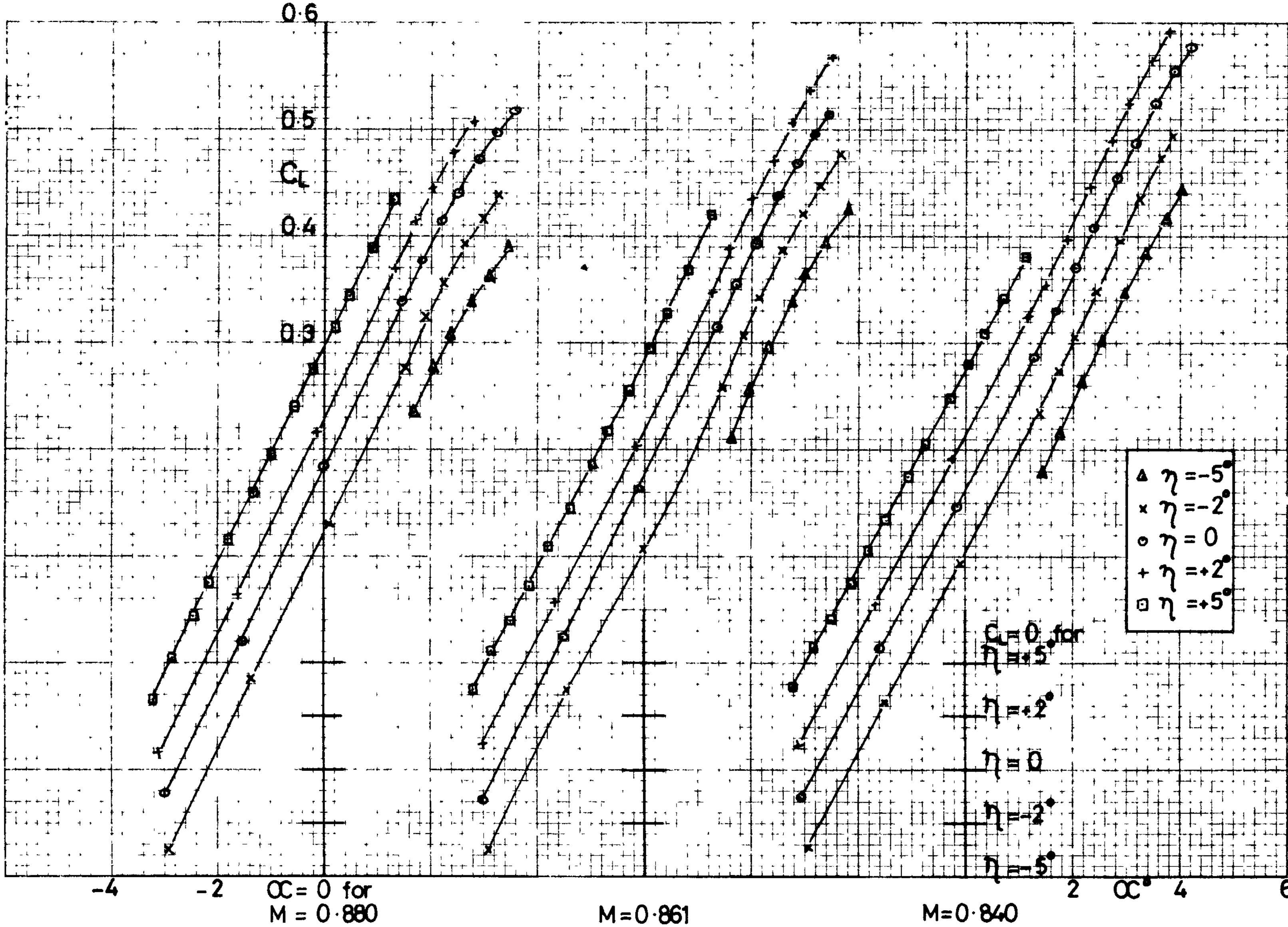

FIG. 3b. $C_L \sim \alpha$.

FIG. 3b.

FIG. 3c. $C_L \sim \alpha$.

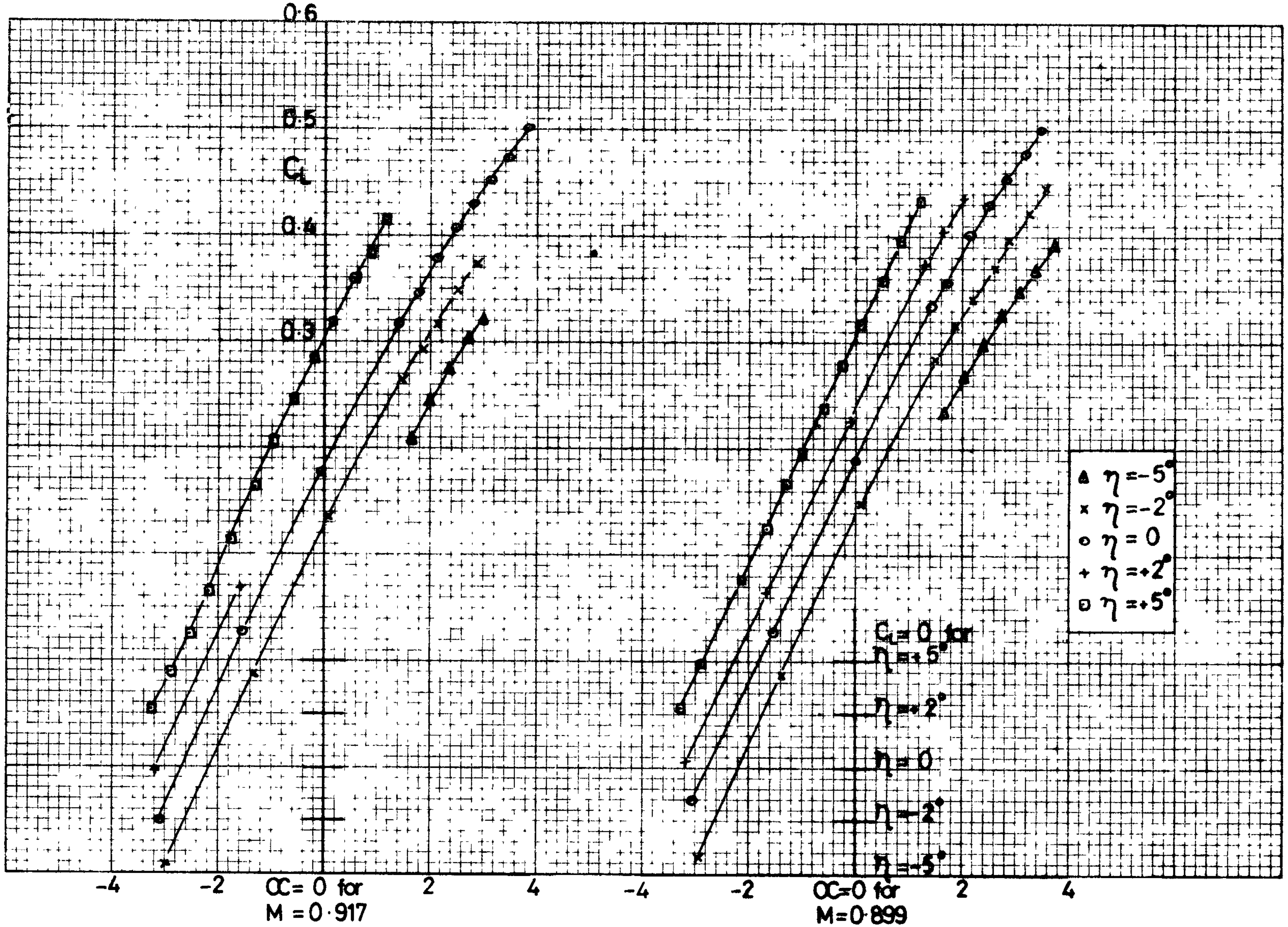

FIG. 3c.

FIG. 4a.

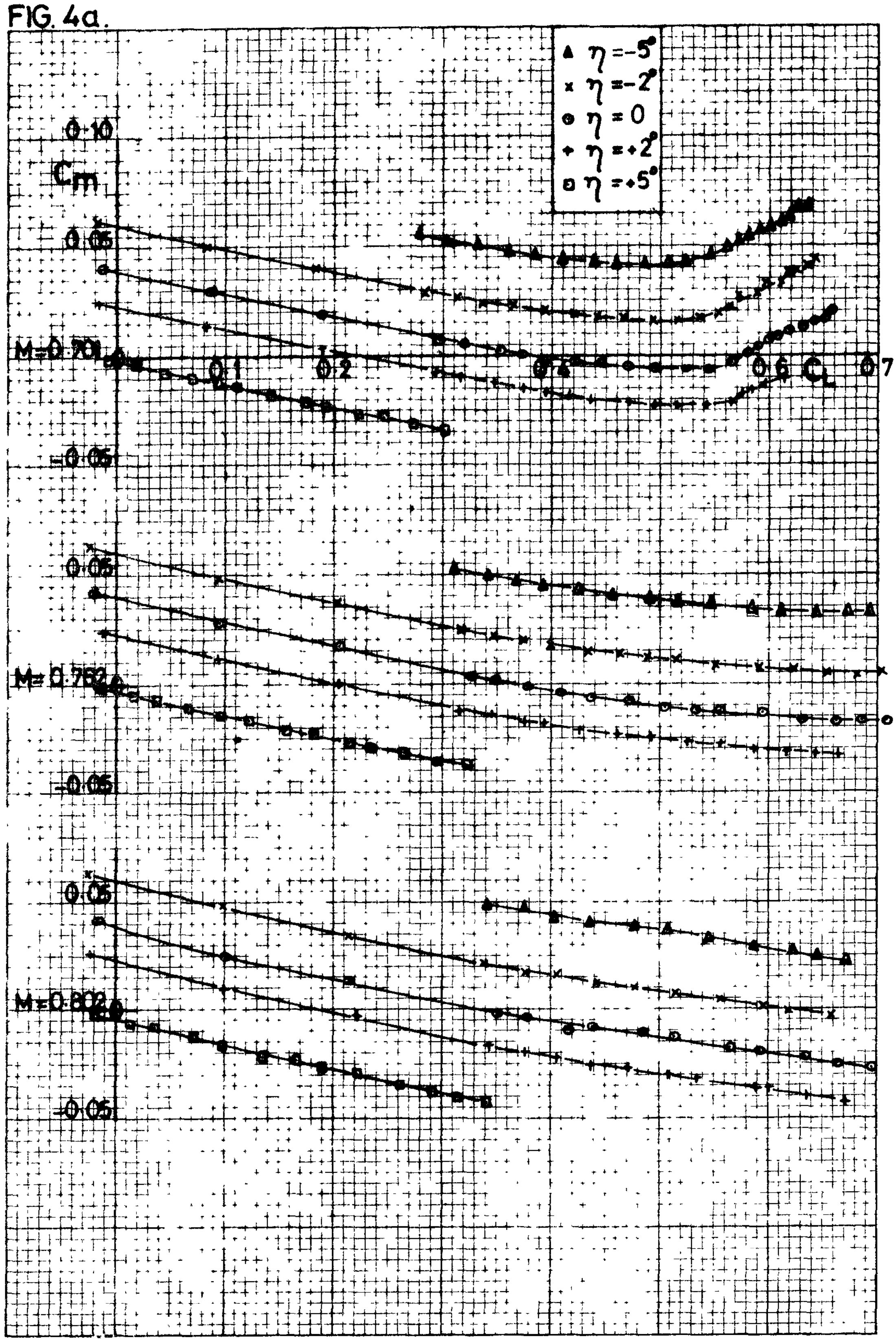

FIG. 4 a. $C_m \sim C_L$.

FIG. 4b.

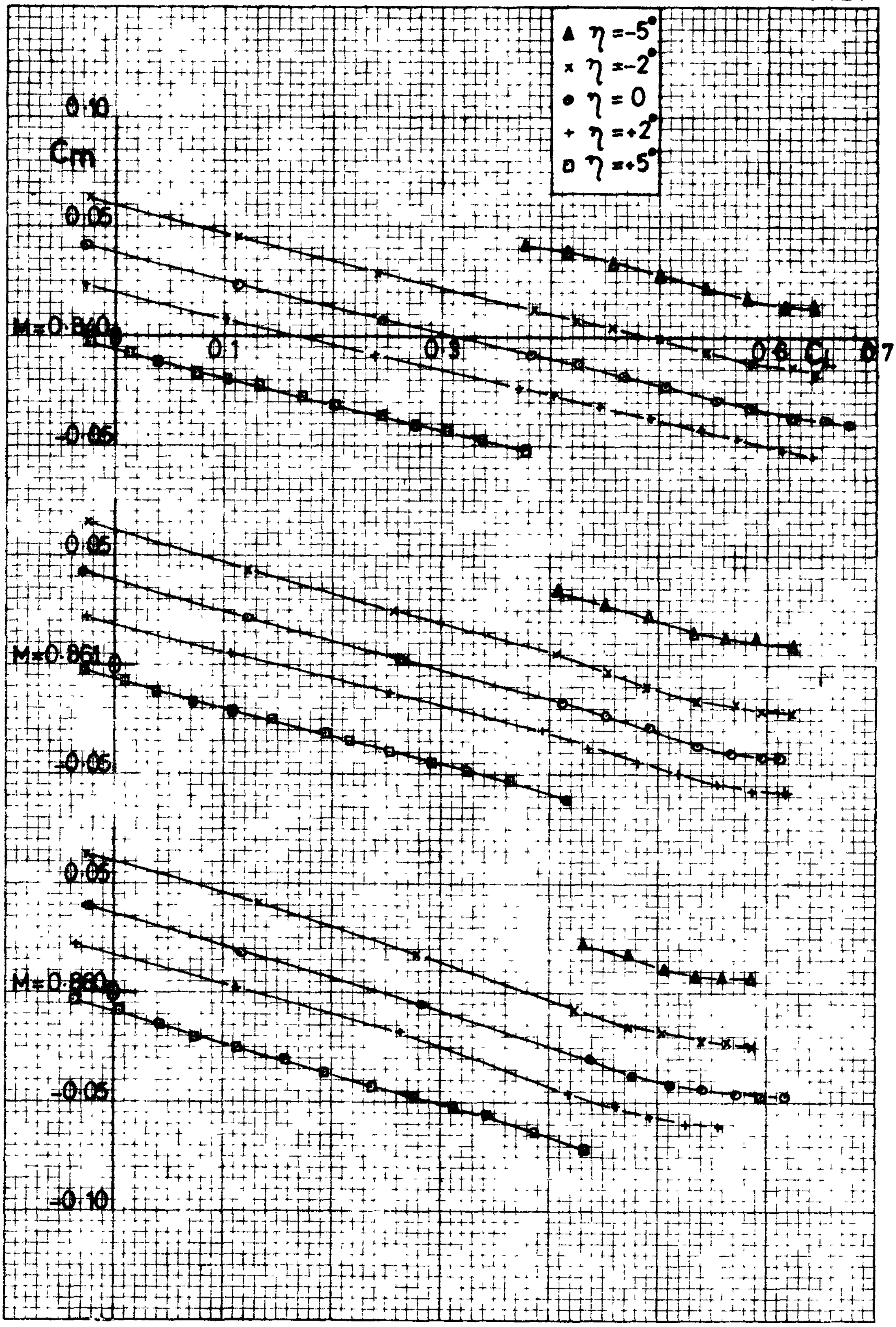

FIG. 4b. $C_m \sim C_L$.

FIG. 4c.

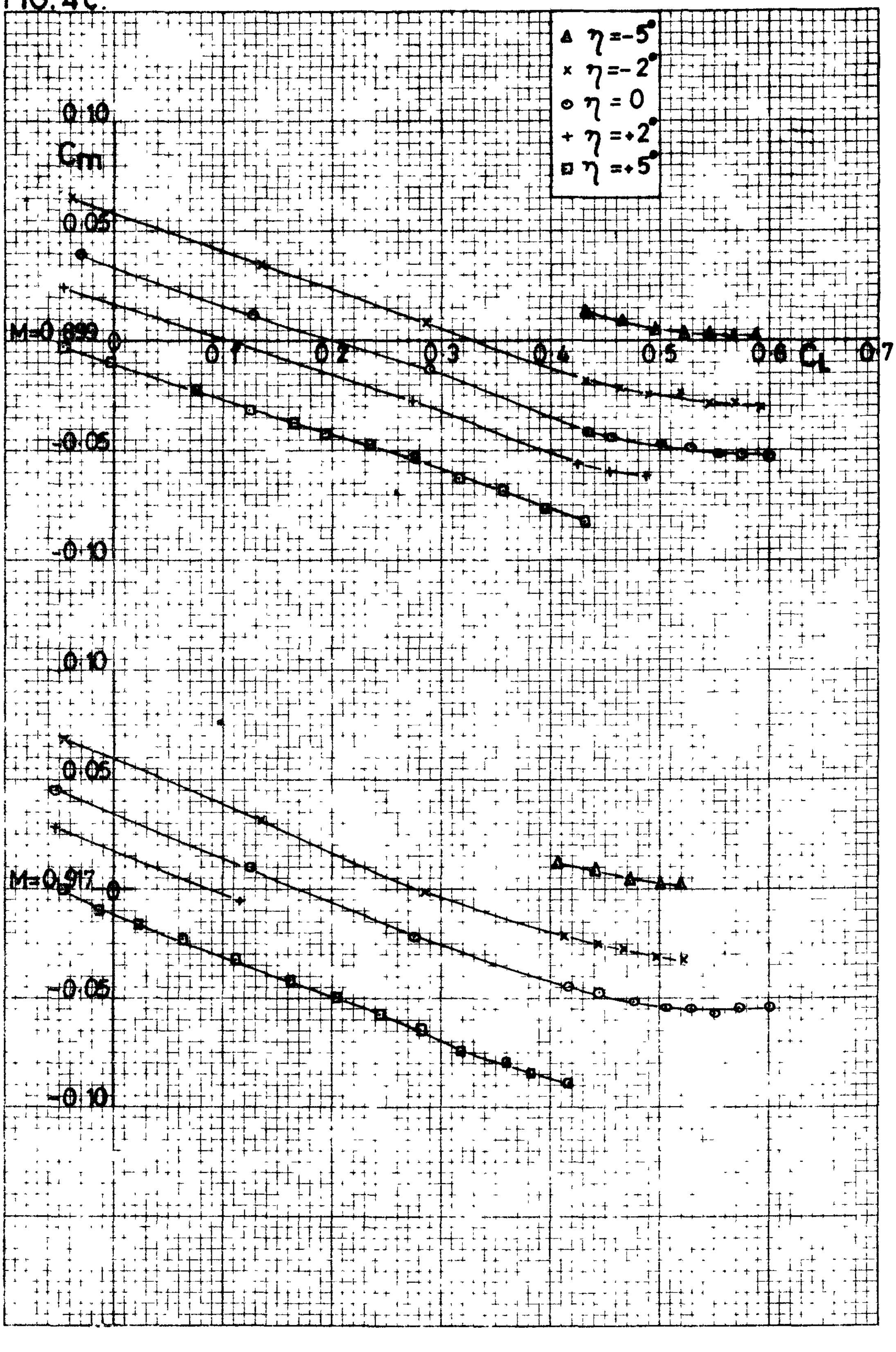

FIG. 4c. $C_m \sim C_L$.

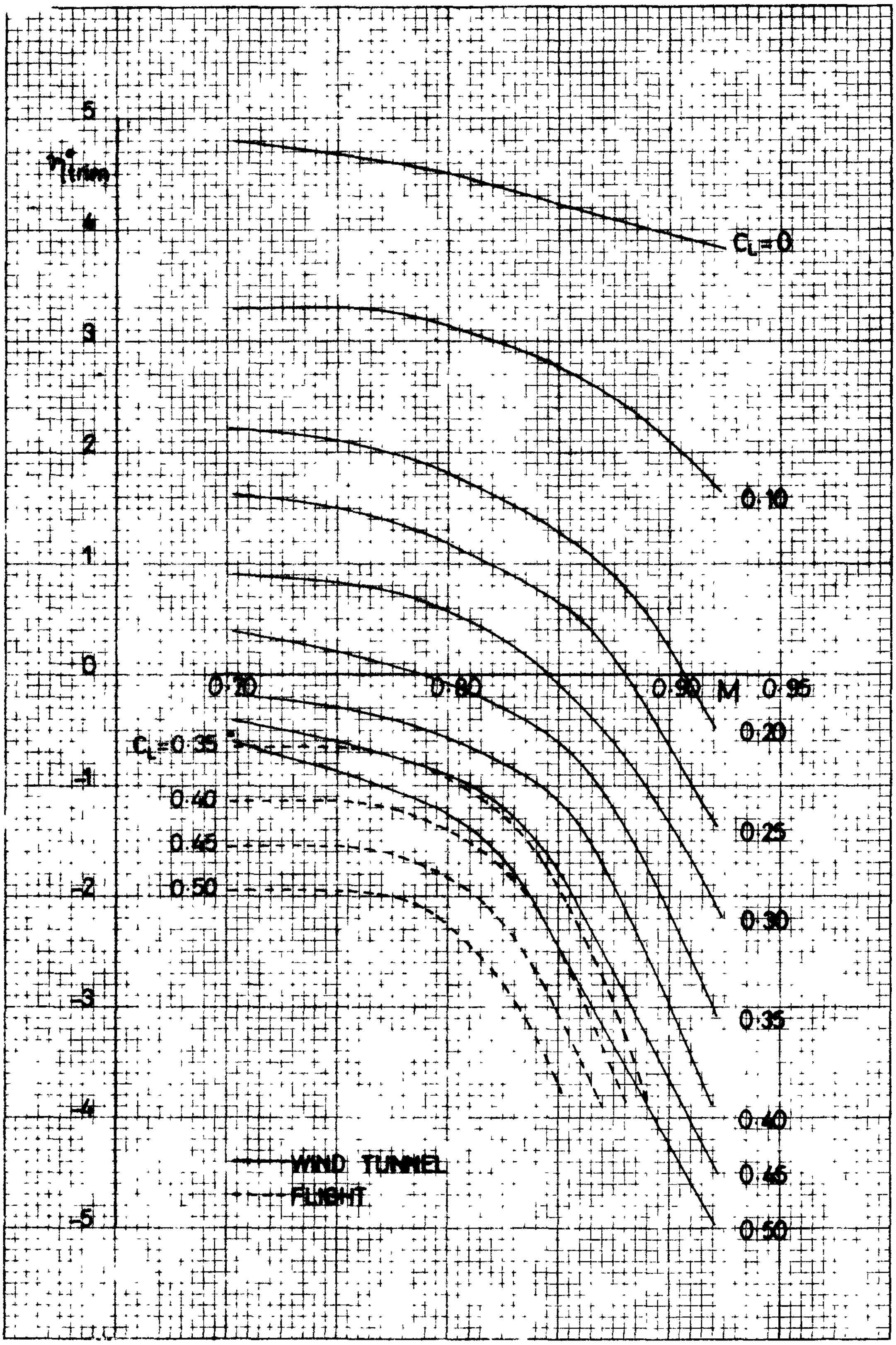

FIG 5. $\eta^\circ_{trim} \sim M$. COMPARISON OF WIND TUNNEL AND FLIGHT ELEVATOR ANGLES TO TRIM.

FIG. 6

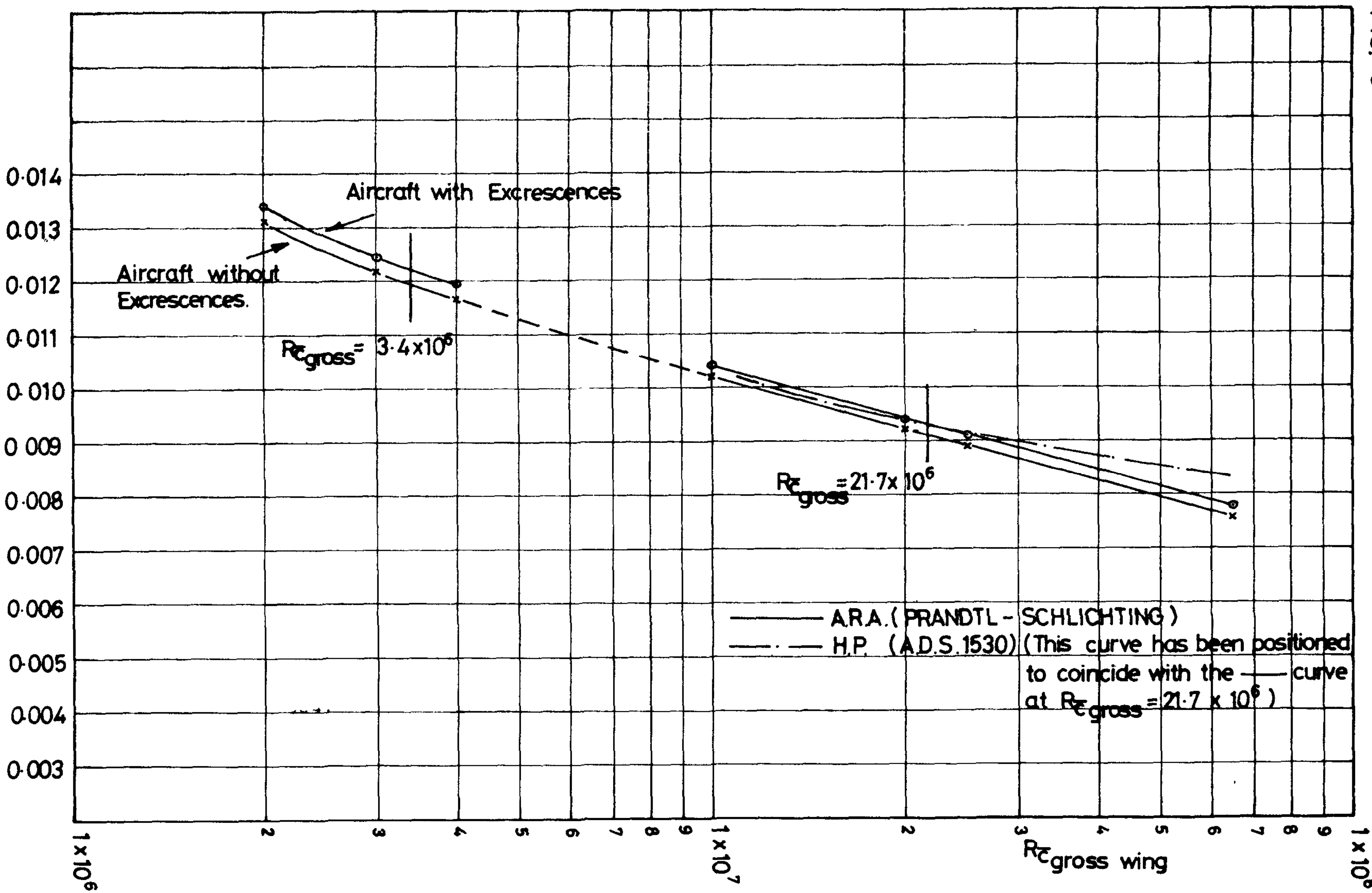

ESTIMATED PROFILE DRAG VARIATION WITH REYNOLDS NUMBER.

FIG. 6

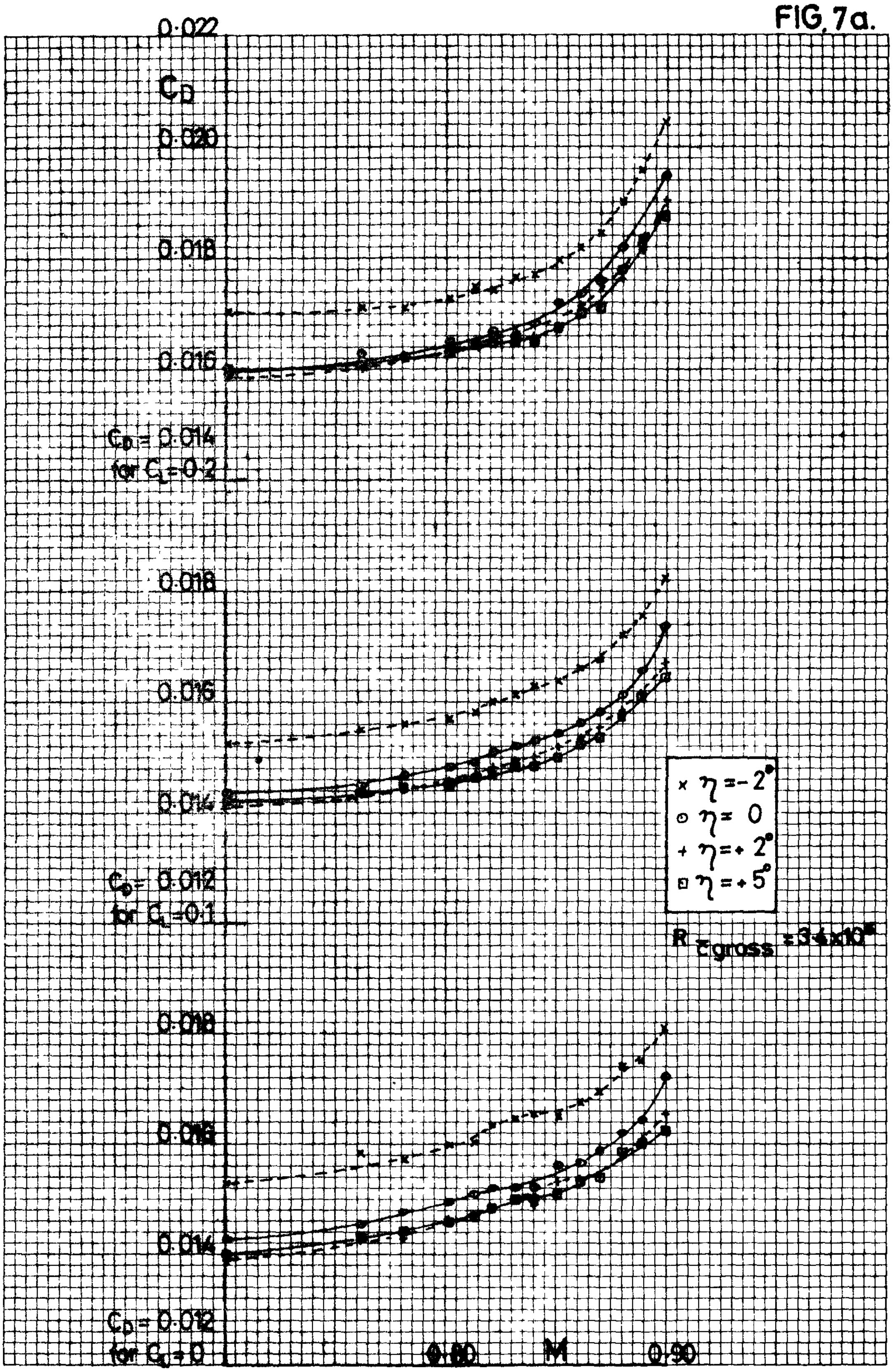

FIG. 7a. $C_D \sim M$ EFFECT OF ELEVATOR ANGLE.

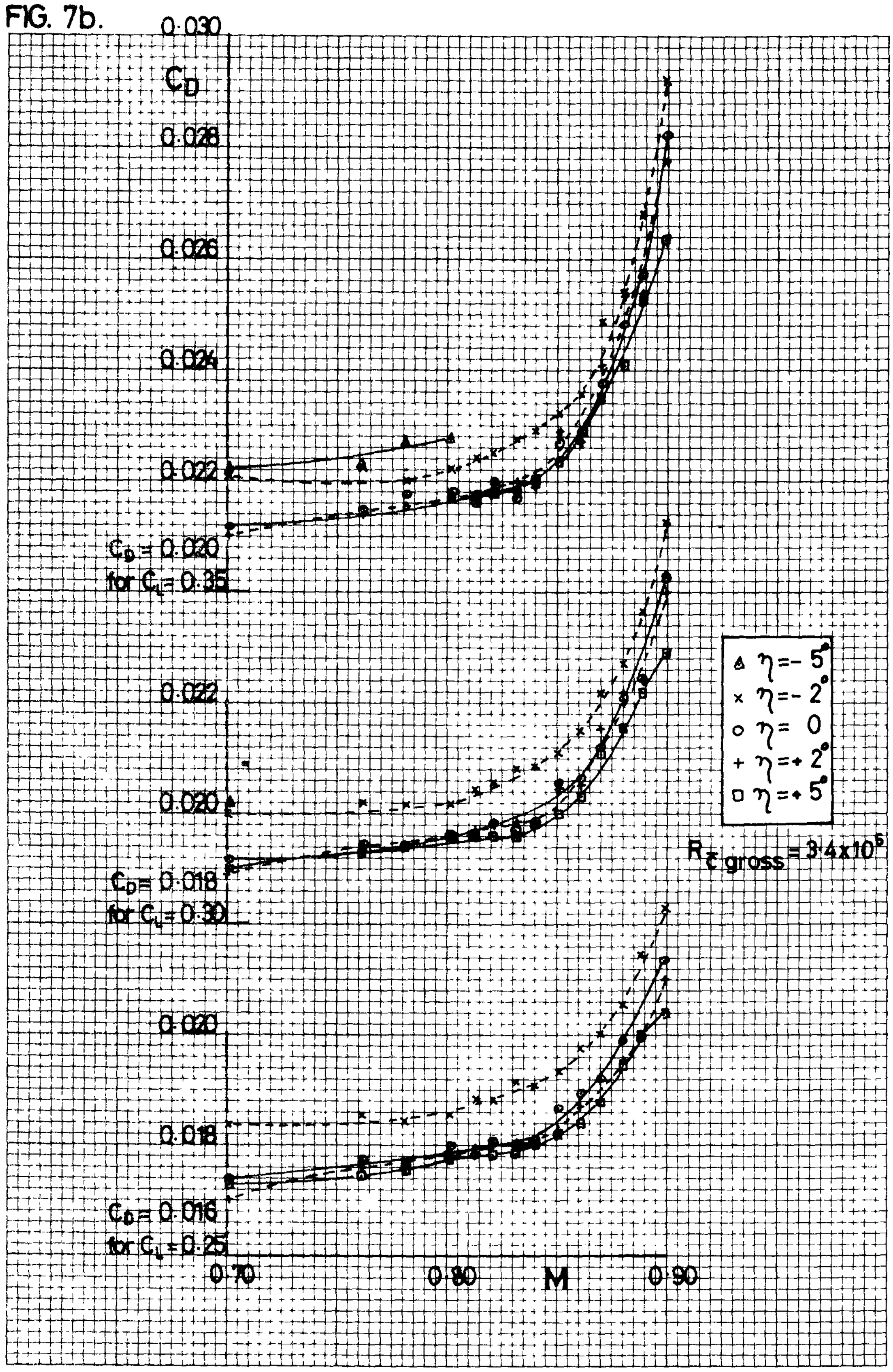

FIG. 7b. $C_D \sim M$

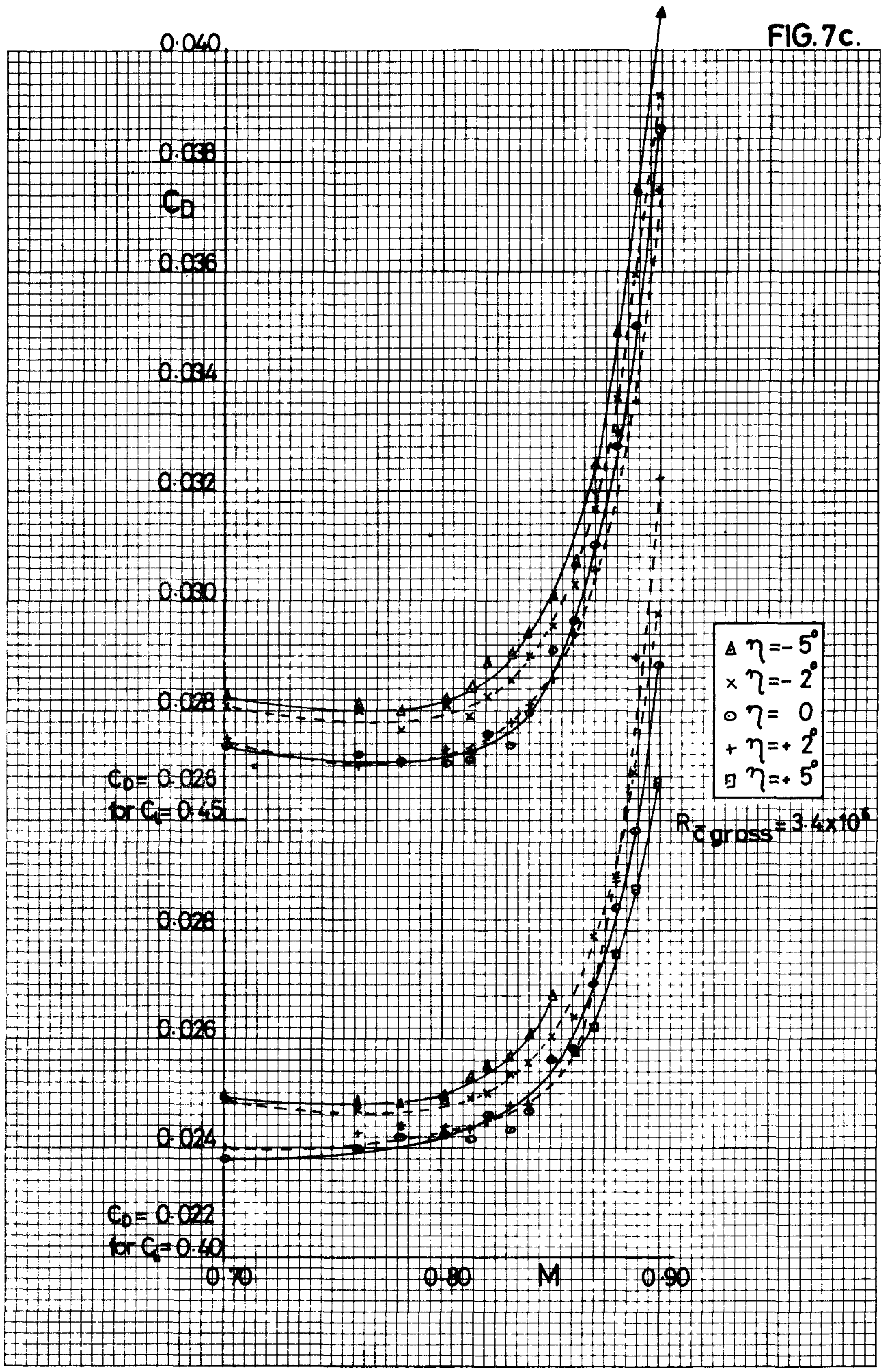

FIG. 7c. $C_D \sim M$.

FIG. 7d,

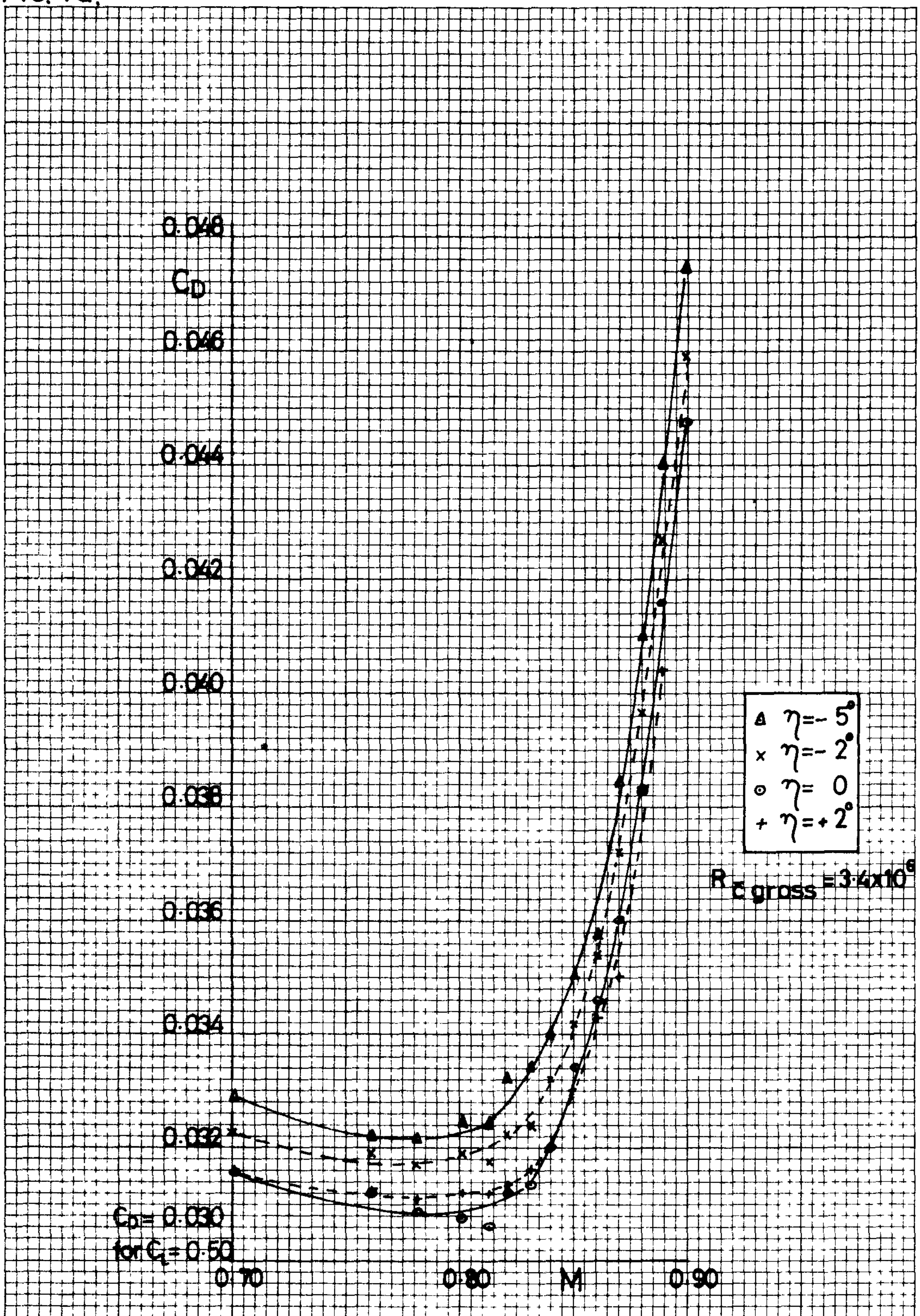

FIG 7d. $C_D \sim M$.

FIG. 8.

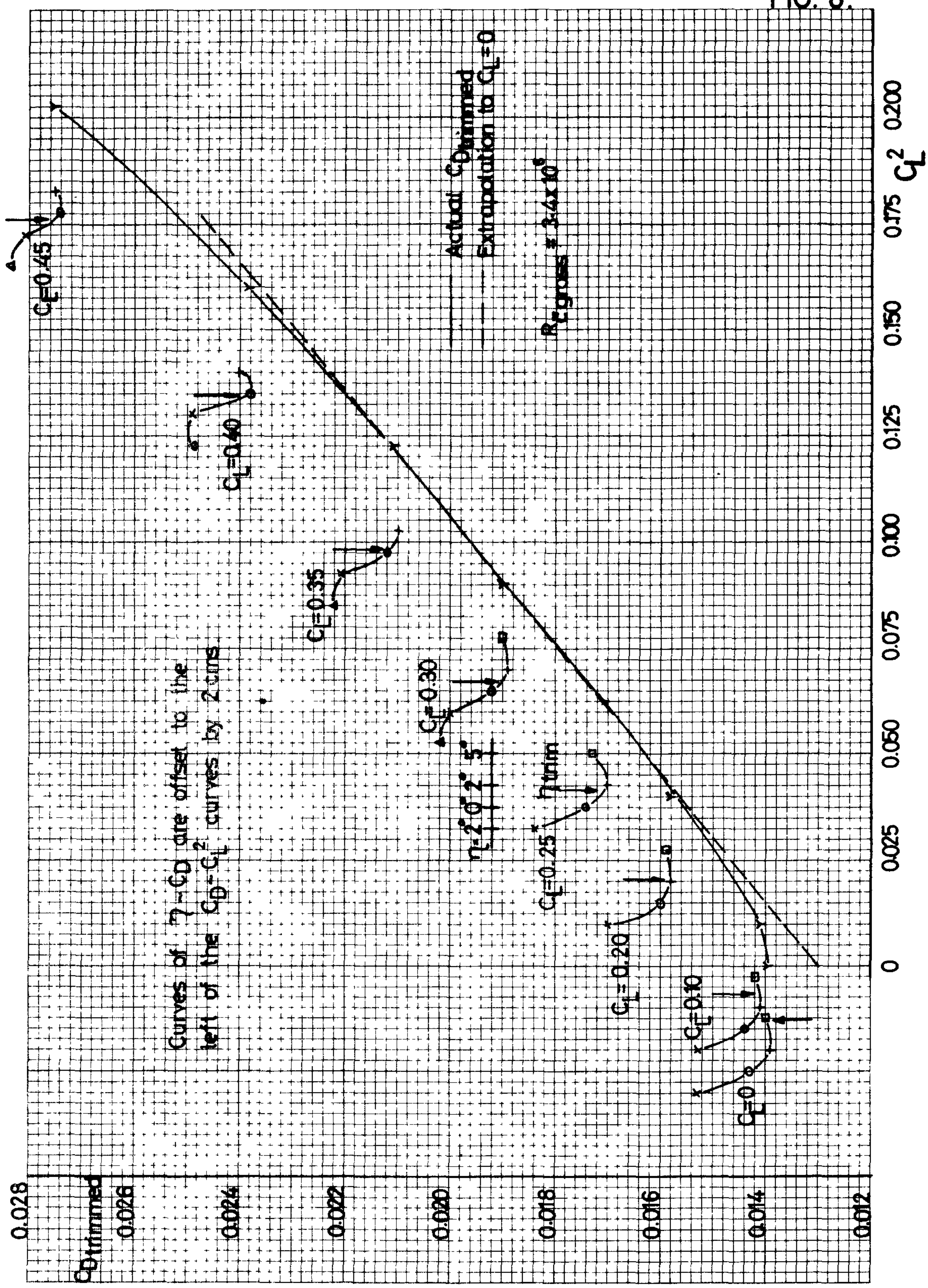

FIG. 8 $C_{D_{trimmed}} \sim C_L^2$ DERIVATION AND EXTRAPOLATION OF CURVES AT M = 0·70

FIG. 9.

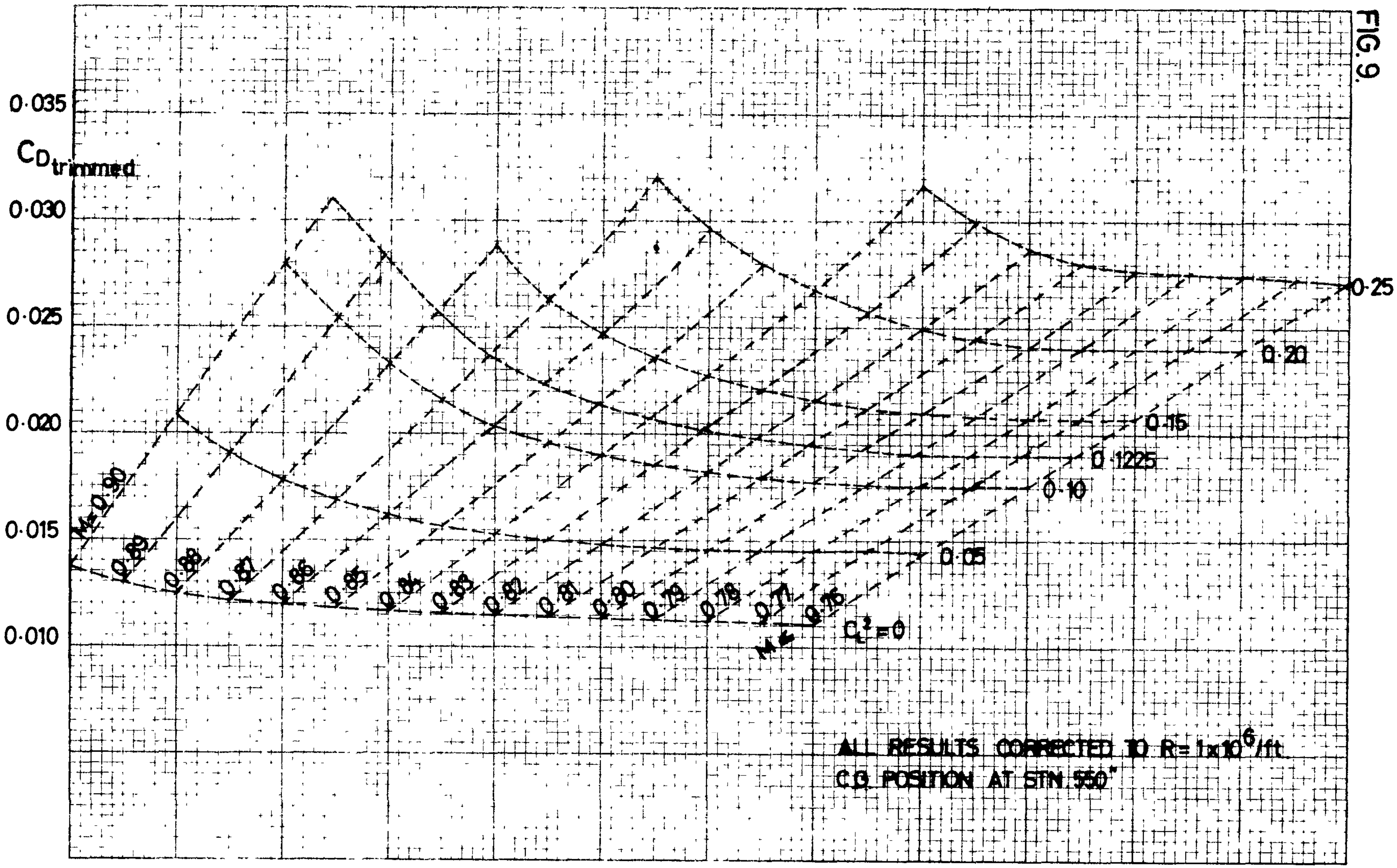

FIG. 9. FULL SCALE AIRCRAFT DRAG.

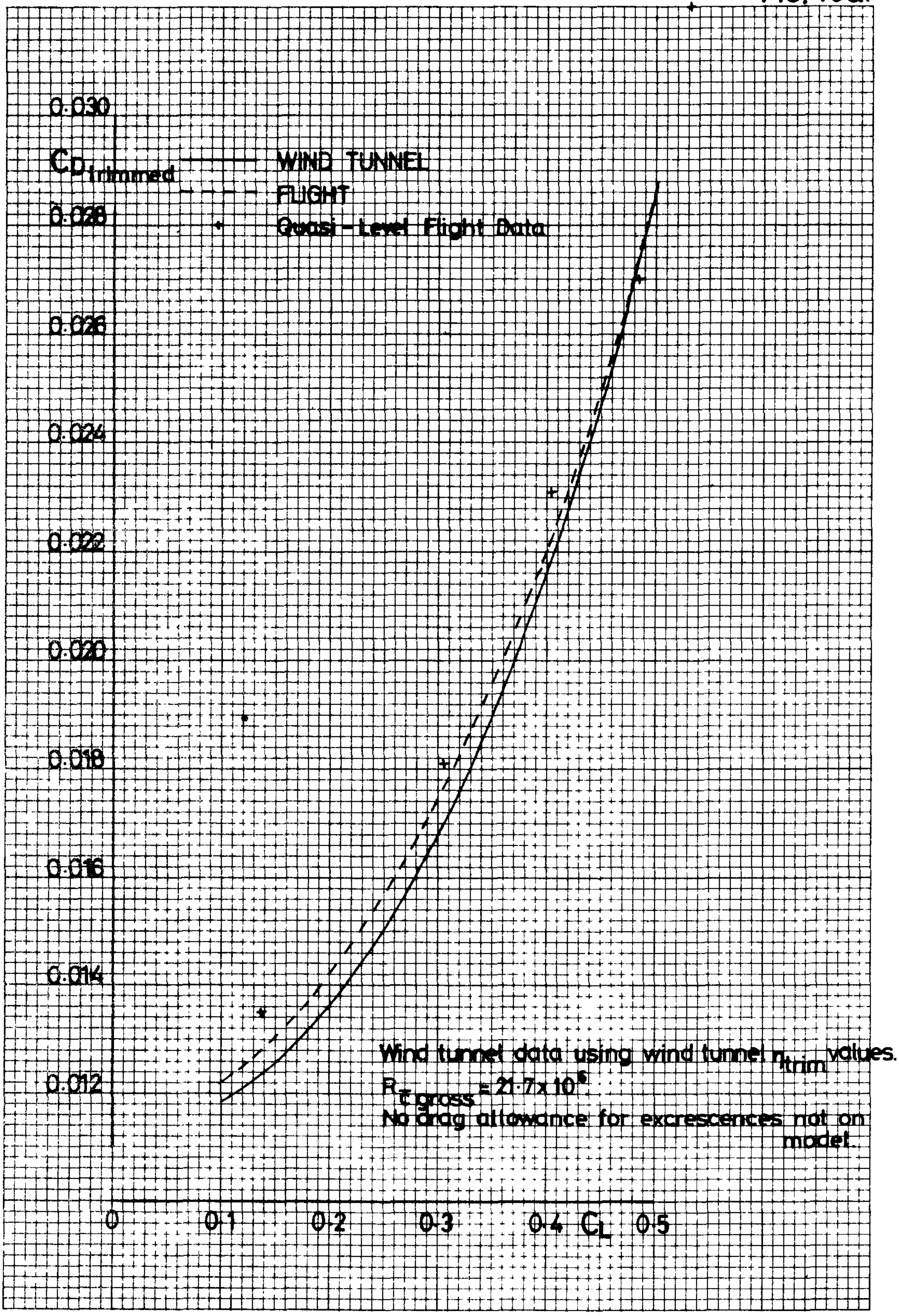

FIG. 10a. $C_{D_{trimmed}} \sim C_L$. COMPARISON OF WIND TUNNEL AND FLIGHT DATA AT M = 0·819.

FIG. 10 b.

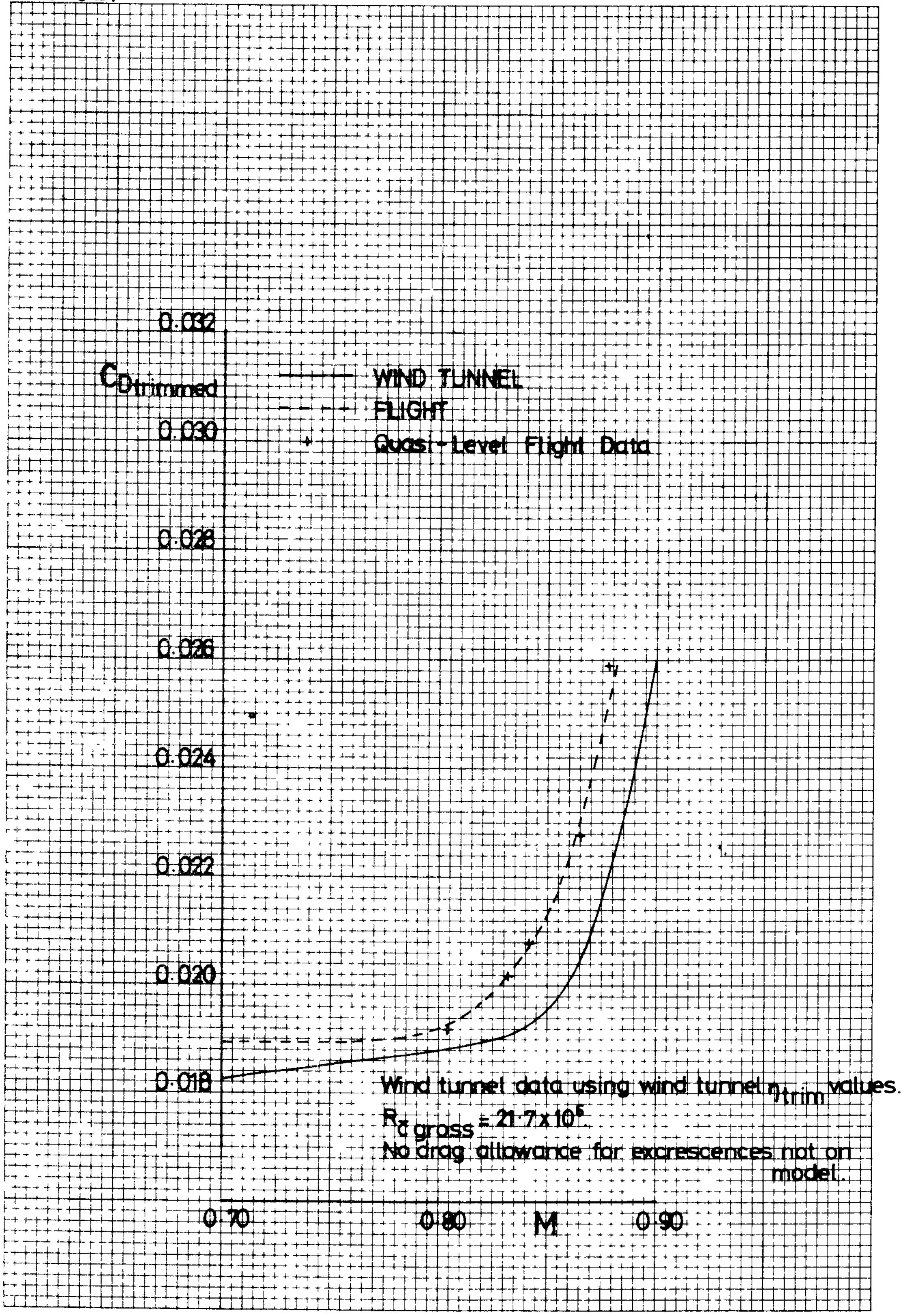

FIG. 10 b. $C_{D_{trimmed}} \sim M$. COMPARISON OF WIND TUNNEL AND FLIGHT DATA AT $C_L = 0 \cdot 35$.

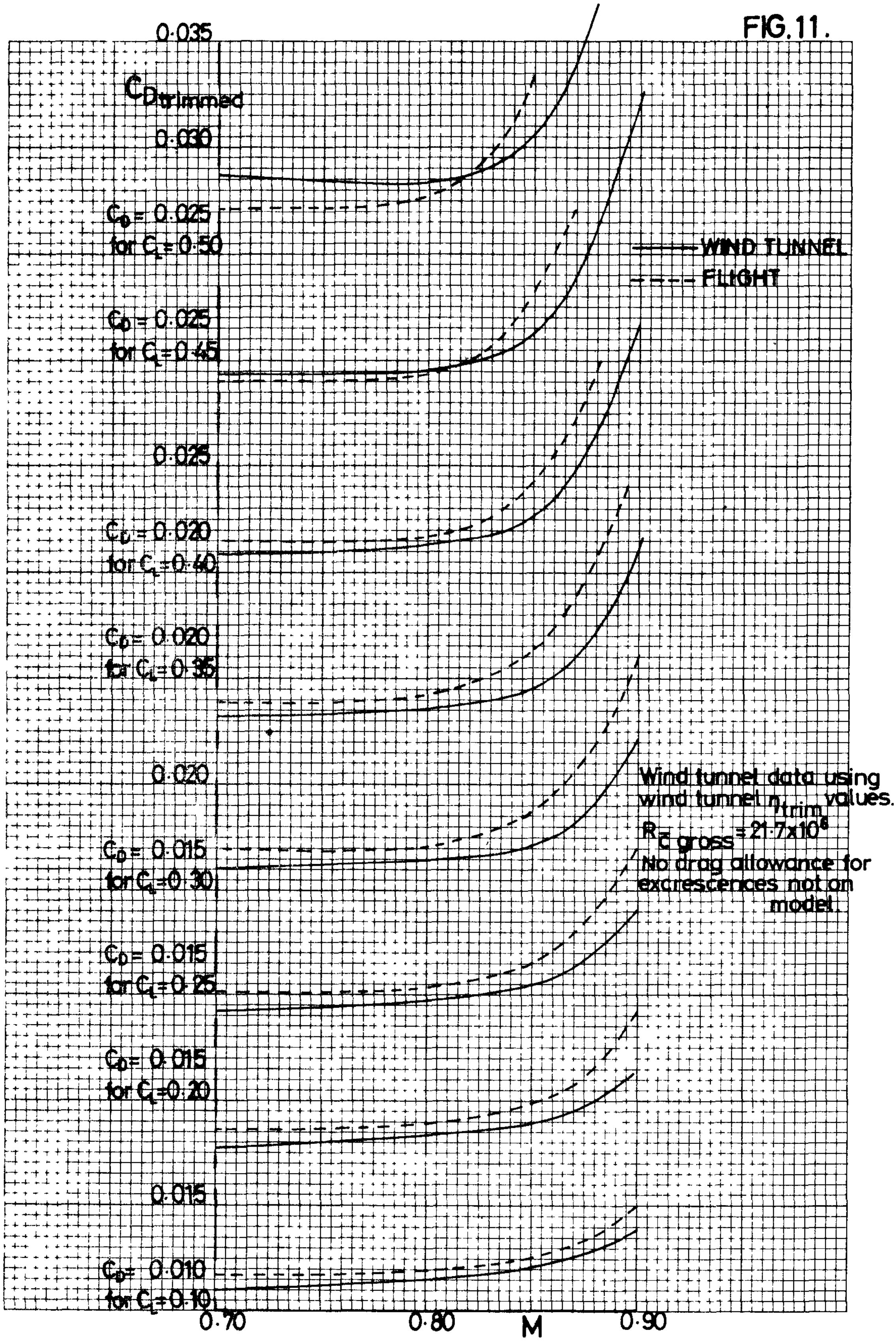

FIG. 11. $C_{D_{trimmed}} \sim M$. COMPARISON OF WIND TUNNEL AND FLIGHT TRIMMED DRAGS.

C.P. No. 1283

HER MAJESTY'S STATIONERY OFFICE

Government Bookshops

49 High Holborn, London WC1V 6HB
13a Castle Street, Edinburgh EH2 3AR
41 The Hayes, Cardiff CF1 1JW
Brazennose Street, Manchester M60 8AS
Southey House, Wine Street, Bristol BS1 2BQ
258 Broad Street, Birmingham B1 2HE
80 Chichester Street, Belfast BT1 4JY

Government publications are also available through booksellers

C.P. No. 1283

ISBN 011 470867 3